

國立臺灣大學理學院大氣科學研究所



碩士論文

Graduate Institute of Atmospheric Sciences

College of Science

National Taiwan University

Master Thesis

灌溉的濕化與冷卻作用對於近地表微氣候的綜合反應

Integrated Responses of Irrigation Moistening
and Cooling Effects to the Near-Surface Microclimate

葉亭佑

Ting-Yu Yeh

指導教授：羅敏輝 博士

Advisor: Min-Hui Lo, Ph.D.

中華民國 112 年 1 月

Jan, 2023

誌謝



能完成一篇碩士論文，其實需要的耐力以及膽量是真正投入研究後才懂的。一路走來，無論是學校方面或是大氣系的老師們都給予我莫大的幫助。首先，我要感謝敏輝老師一路的栽培我，第一次與老師多次交流是在製作統計投影片，到後續碩士班多次 meeting 的交流，都感受到老師的學識淵博與對學生的關愛，讓我在大氣系的研究路途上不僅學習到大量的陸氣交互知識，老師也給我很多勇氣繼續往前前進。這份勇氣得來不易，讓我有機會提出我的見解，有機會在腦中思辨，更有機會踏進大公司實習，這份恩情實在難以言喻。或許我的誌謝在論文庫的茫茫大海中如同一根細針，但這份感謝在我心中佔有不可或缺的地位。

另外我也要感謝研究室的夥伴們，在專題討論前給予我很多有意義且實質的勘誤與想法，也協助我模式的輸出，若沒有大家的幫助，這篇論文將會漏洞百出且內容簡陋。我還要謝謝鴻基老師，在我碩一時期的照顧，當年的一字一句的推導淺水方程式，都化為我後續對於研究的數學基礎，碩一時的學長姐也是對我如家人般的呵護，實為感動，希望在美國與氣象局發展的你們，都能成為未來的閃亮之星。

最後我要感謝我的家人，有你的陪伴才有今天的我，住在雨都的我們，冬季是如此的寒冷，但我們的心卻是永遠在一起，面對歡笑與淚水，一起把我送出社會。

亭佑謝謝你，你無所畏懼的，完成你的心願。

中文摘要



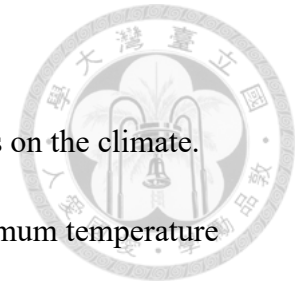
近年來許多研究探討灌溉導致近地表微氣候改變的程度，但目前尚未有文獻提出在乾濕季下，濕球溫度對於溫度及濕度改變的敏感度，且至今尚未了解灌溉對濕球溫度氣候平均態的影響。本文探討灌溉的冷卻效果與濕化作用對於濕球溫度的互補關係以及乾濕季下濕球溫度的改變特徵。前人已發現一年中最熱月份的平均最高溫隨著灌溉的擴大而降溫（冷卻效果），而濕化效果主要是強調灌溉增濕近地面空氣將提升濕球溫度與降低該地區的舒適度，本文將探討此兩大作用並結合不同的背景濕度條件，討論濕球溫度變化的主導因素。此研究分析美國國家大氣研究中心(National Center for Atmospheric Research)發展之耦合氣候模型(Community Earth System Model)以及非耦合之陸地模型(Community Land Model)所輸出的兩公尺高的日最高溫、日平均相對濕度與混合比，並計算該地區的濕球溫度。我們同時使用多重變數線性回歸技術從多重訊號中分離出單一強迫項，得出冷卻效應與濕化效應各自對濕球溫度的影響。

灌溉比例在美國中部、歐洲、南亞與華北地區在過去百年有顯著擴大，模型分析結果發現隨著灌溉範圍擴張，所有地區的最高乾球溫度皆下降。在分析影響濕球溫度的因子後，發現混合比對於濕球溫度較為敏感。本研究總結兩種情形，如果背景相對濕度較低時，則灌溉的濕化效果較高，可能會主導濕球溫度上升的過程。另外，如果背景相對濕度接近飽和，因為蒸發機制不顯著，導致灌溉冷卻與濕化效應無顯著發生，進而對濕球溫度無顯著影響。由於暖化下的氣候平均態改變，會改變灌溉的效應，因此未來討論乾季濕熱之熱傷害，需同時考量到灌溉與暖化下的共同效應。

關鍵字：灌溉、濕球溫度、濕化效應、冷卻效應、熱傷害、混合比。



Abstract



Irrigation practices can have significant biogeophysical effects on the climate. Previous studies have shown that the change in average daily maximum temperature during the hottest month of the year has warmed less in regions with irrigation expansion in the past 100 years. Furthermore, the irrigation's moistening effect may cause higher wet-bulb temperature due to higher near-surface water vapor from excess evaporation. However, the effects that dominate the change of the wet-bulb temperature in the dry and wet seasons are not well understood. This study investigates the competing effects of cooling and moistening on the wet-bulb temperature. We use the meteorological variables of daily maximum temperature (T2m); daily mean relative humidity (RH) and daily mean surface pressure are used to calculate the specific humidity (or mixing ratio) and wet-bulb temperature from NCAR CESM coupled climate model and the offline NCAR Community Land Model. The linear regression technique isolates an individual forcing from a lumped signal and analyzes the temperature change through irrigation cooling and moistening effects. The irrigation fraction expanded in the central USA, Europe, South Asia, and North China in the past 100 years, so the maximum temperature decreased over those regions. We further differentiate the wet-bulb temperature from the dry-bulb temperature and the mixing ratio, which is very sensitive when the mixing ratio changes. The results show that when the background relative humidity is low, the mixing ratio could change a lot, which means the amount of mixing ratio change has a

high probability of staying in the dominant region. The wet-bulb temperature is non-linear with the T and RH. We conclude with two scenarios. If background RH is low, the irrigation moistening effect most likely dominates. On the other hand, if the background RH is high, the evaporation is less from the lower water gradient.

Therefore, there is no apparent cooling or moistening effect to alter the wet-bulb temperature. In a nutshell, irrigation can worsen comfort and increase the danger of heat stress, especially in dry conditions. This is an essential factor needed to be considered in the future.

Keywords: Irrigation, Wet-bulb temperature, Moistening effect, Cooling effect, Heat stress, Mixing ratio.

Contents



誌謝.....	i
中文摘要.....	ii
Abstract.....	iv
Contents.....	vi
List of Tables.....	viii
List of Figures.....	ix
Chapter 1. Introduction.....	1
1.1 Irrigation cooling effect.....	1
1.2 Wet-bulb temperature.....	3
1.3 Scientific questions and hypotheses.....	6
Chapter 2. Data of the coupled climate model and method.....	8
2.1 Data.....	8
2.2 Method.....	10
Chapter 3. Results of coupled climate model.....	13
3.1 Global land.....	13
3.2 Central USA.....	16
3.3 North China.....	17
3.4 Europe.....	18
3.5 South Asia.....	18
Chapter 4. Results of the offline land surface model.....	25

4.1 Data.....	25
4.2 Comparison between offline and coupled model.....	26
4.3 The scatter plot in South Asia.....	27
4.4 The diurnal difference in the dry and wet seasons (South Asia).	28
4.5 The yearly trend of wet-bulb temperature in South Asia and North China.....	29
Chapter 5. Discussion.....	33
Chapter 6. Conclusions.....	37
Chapter 7. References.....	39





List of Tables

Table 1. CESM simulation production.44



List of Figures

- Figure 1.** Observed warming rates affected by irrigation. Boxplots of the total (ΔTX_m , a, b) and irrigation-induced ($\Delta TX_{m_{irr}}$, c, d) change in average daily maximum temperature during the hottest month of the year for global land (a, c) and South Asia (b, d) between 1901 and 1930 and 1981 and 2010. This figure and legend are taken from Wim et al. (2020) figure 1.45
- Figure 2.** Irrigation driven cooling in the Indo-Gangetic Plain. This figure and legend are taken from Vimal et al. (2020) figure 1.46
- Figure 3.** Change in probability of hot extremes from expanding irrigation and other forcings. This figure and legend are taken from Wim et al. (2020) figure 2.47
- Figure 4.** (a) Relationship between human mortality and area affected by extreme dry and moist heat stress (%) in India with 3-day maximum T_w greater than 27 during the heatwave. (c) same as (a) but for 3-day maximum T_2 greater than 45. Mortality data was obtained from EM-DAT (<https://www.emdat.be/>) for the 1979-2016 period. This figure and legend are taken from Vimal et al. (2020) figure S6.48



Figure 5. Spatial distribution of highest daily maximum wet-bulb temperature in modern record (1979-2015). This figure and legend are taken from Im et al. (2017) figure 1.49

Figure 6. T_{wmax} ($^{\circ}C$), and maps of the ensemble averaged 30-year T_{wmax} . This figure and legend are taken from Im et al. (2017) figure 2.50

Figure 7. The role of irrigation on summer heat fluxes, temperature humidity SLP, and PBL height. This figure and legend are taken from Vimal et al. (2017) figure 3.51

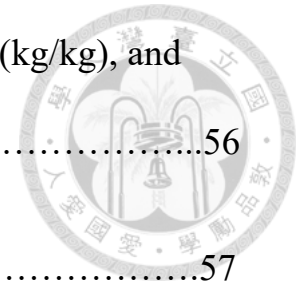
Figure 8. Changes in three days maximum heat indicators in India during April to May for 1979 to 2018 period. This figure and legend are taken from Vimal et al. (2017) figure 2.52

Figure 9. Isopleths of T_w versus RH% and T. This figure and legend are taken from Roland et al. (2011) figure 2.53

Figure 10. Irrigation fraction difference (%) between the early 20th century reference period (1901-1930) and present-day (1981-2010).54

Figure 11. Change in ΔTX_m versus change in the irrigated fraction in Global land, South Asia, North China, and the Central USA.55

Figure 12. Change in temperature (K), specific humidity (kg/kg), and maximum wet-bulb temperature (K) in global land.	56
Figure 13. Same as figure 12, but for Central US.	57
Figure 14. The equivalent effect of increasing mixing ratio on dry-bulb temperature change.	58
Figure 15. Same as figure 12, but for North China.	59
Figure 16. Same as figure 12, but for Europe.	60
Figure 17. Same as figure 12, but for wet seasons in South Asia.	61
Figure 18. The specific humidity (kg/kg) changes due to other forcing.	62
Figure 19. Same as figure 12, but for dry seasons in South Asia.....	63
Figure 20. Irrigation effect of one month average in dry South Asia (1981-2010). The criteria are RH lower than one standard deviation. ...	64
Figure 21. Same as figure 20, but the criteria are RH higher than one standard deviation which represents as wet South India.	65
Figure 22. The probability density function of (a) temperature change (K), (b) mixing ratio (kg/kg), (c) latent heat flux (W/m^2) in wet and dry conditions.	66
Figure 23. Comparison between the coupled and offline models in daily maximum and minimum in South Asia.	67



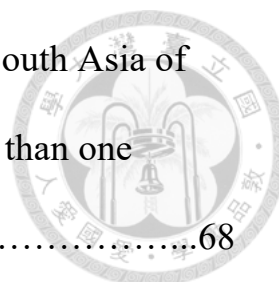


Figure 24. Irrigation effect of one month average in wet South Asia of the offline model (1906-2014). The criteria are RH higher than one standard deviation.68

Figure 25. Same as figure 24, but the criteria are RH lower than one standard deviation which represents dry South India.69

Figure 26. The probability density function of (a) mixing ratio change, (b) temperature in wet (blue line) and dry seasons (red line).70

Figure 27. Each variable difference due to irrigation from 1906 to 2010 in the dry season of South Asia.71

Figure 28. The same as figure 27, but for the wet season in South Asia.72

Figure 29. Variables difference affected by irrigation in South Asia.73

Figure 30. The same as figure 29, but for North China.74

Figure 31. The specific humidity of different layers in North China over time.75

Figure 32. South Asia profile in 1981-2010 for dry and wet seasons in control run and the difference between irrigation and control analysis.76

Figure 33. The summary of wet and dry conditions of wet-bulb temperature.	77
Appendix A1. The probability density function of dry and wet events from January to March in South Asia. The blue and red lines represent the wet and dry conditions.	78
Appendix A2. Same as A1, but for April to June.	79
Appendix A3. Same as A1, but for July to September.	80
Appendix A4. Same as A1, but for October to December.	81





Chapter 1. Introduction

1.1 Irrigation cooling effect

Irrigation practices have a large geophysical effect on climate (Wada et al., 2013).

Researches show that the temperature can be affected by evaporation, which is a cooling effect and especially in highly irrigated regions (Chou et al., 2018). These cooling effects can be investigated by observation data and CESM model simulations.

Wim et al. (2020) investigated the expansion of irrigation and found a negative correlation between daytime summer temperatures and irrigation extent. The mechanism comes from adding water to soil makes it moisturized. Then, evaporation takes heat away and the temperature drops. Figure 1 shows the change in average daily maximum temperature during the hottest month of the year, named, which has warmed less with irrigation expansion. The delta symbol represents the difference between 1901-1930 and 1981-2010. Figure 1a explains the ΔTXm in all forcing scenarios.

When the change in irrigated fraction increases, ΔTXm decreases. Also, when the x-axis number is small, ΔTXm is larger than zero. This signal comes from anthropogenic warming. To get the irrigation effect, Wim et al. (2020) used the regression technique to distinguish a lumped signal from all forces. Figure 1c shows that irrigation is a cooling

effect. The more changes in irrigated fraction, the lower the temperature difference becomes.



In South Asia, Indo-Gangetic is a classical area to investigate the effect of irrigation. Vimal et al. (2020) found the heat stress in highly irrigated areas decreased by the cooling effect using in situ observations, reanalysis, and high-resolution Weather Research and Forecasting (WRF) model driven by ERA5 with and without irrigation. In figures 2a and 2b, the irrigation hot zone is located in the red contour which is cooler than other places influenced by global warming. In figure 2d, the surface temperature gets lower, when the irrigated area gets higher.

It is becoming difficult to ignore the effect of global warming and extreme events. Wim et al. (2020) also explored the probability of hot extremes in 3 kinds of scenarios: all forcing without irrigation, irrigation, and all forcing. Figure 3 displays the probability ratio of over the 99th percentile of high temperature. In these figures, note that irrigation is an alleviated factor in the hot extreme, especially in Indo-Gangetic Plain. Therefore, almost all regions suffer from a high probability of hot extremes because of global warming except for Indo-Gangetic Plain. According to their simulation, around one billion people were less exposed to high temperatures due to the

irrigation cooling effect.




1.2 Wet-bulb temperature

More and more researchers highlight the mortality attributed to the heat wave. For instance, Vicedo et al. (2021) found that 37.0% of heat-related deaths are related to anthropogenic climate change, which it is significant in every continent. They use the cutting-edge time-series regression to get the relationship between mortality and temperature at 731 stations, then project to the natural-only scenario. In this study, they don't apply specific humidity in their regression.

On the other hand, Vimal et al. (2020) calculated the mortality using dry-bulb temperature and wet-bulb temperature in India as figure 4. The correlation coefficient of mortality over the T_w plot is larger than mortality over the T plot, which means T_w is a better indicator of understanding the linkage between heat stress and mortality in India.

In addition, Steven et al. (2010) argued that a resting human body (except for absorbed solar heating) generates about 100W of metabolic heat that three main processes must carry out, that is, evaporation cooling, heat conduction, and infrared cooling. However, no matter how the object is wet or well-ventilated, the second law of



thermodynamics does not allow the heat to be taken away from an object when the environment T_w is higher than the object's temperature. As far as humans are concerned, humans maintain a core body temperature of about 37°C and the skin temperature must be lower than the core temperature (about 35°C) to take away the metabolic heat (McNab et al, 2002). According to the above discussion, they conclude that humans cannot stay in an environment where T_w is over 35°C for a long period. This is also explored by Dunne et al. (2013), who indicated the wet-bulb temperature could also affect the labor capacity. Besides, Krakauer et al. (2020) conducted climate simulations to show that irrigation not only increases humidity but also worsens heat stress.

Therefore, based on Steven's idea, Im et al. (2017) plot the spatial distribution of the highest daily maximum wet-bulb temperature which is defined as 6 hours window average. Most of the high T_w is located in Asia. They show that T_w in the Persian Gulf and the Red Sea can get over 31°C , and in Indo-Gangetic can get to 28.5°C , as figure 5. In addition, the above findings are similar to Raymond et al. (2020) using ERA-Interim reanalysis.

Focusing on the Indo-Gangetic area, Im et al. (2017) projected the daily maximum

wet-bulb temperature using Representative Concentration Pathway (RCP) 4.5 and 8.5

(Figure 6). In this figure, $T_{w_{max}}$ in the Indo-Gangetic area might get to 31°C under RCP

4.5 and 35°C under RCP 8.5. That is to say, around 4% of people will experience $T_{w_{max}}$

exceeding 35°C by 2100. However, this effect doesn't exist only in Indo-Gangetic

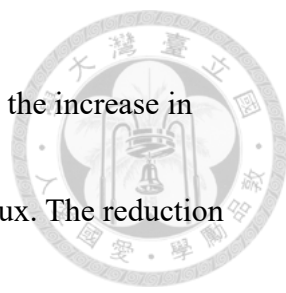
Plain. Kang and Eltahir (2018) conducted a Business-As-Usual (BAU) scenario of

greenhouse gas to show that the wet-bulb temperature would increase by 3.4 (K) under

irrigation run, which is larger than the control simulation by 1 (K) in the North China

Plain.

Vimal et al. (2020) included the idea of wet-bulb temperature and irrigation cooling effect in their study. They calculated the differences in the summer energy budget, temperature, specific humidity, sea level pressure (SLP), and boundary layer height (PBL height). Figures 7a to 7c explain the energy flux changes. Because of more soil water, the evaporation flux goes up and takes away the heat. At the same time, the temperature gradient between surface air and soil decreases. Therefore, sensible heat flux decreases. The energy anomaly goes away from land totally because of the larger flux of evaporation. Thus, increased latent heat flux and evaporation lead to increased evaporation cooling and reduced land surface temperature and 2m temperature.



Moreover, Vimal et al. (2020) proposed a mechanism to explain the increase in specific humidity. As mentioned above, irrigation changes the heat flux. The reduction in sensible heat flux makes surface air cool, and descending air causes an increase in sea level pressure and the development of anticyclonic circulation (figure 7g). Therefore, the PBL collapses (figure 7h) and a shallower PBL leads to an increase in the low-level moist enthalpy and specific humidity (figure 7f). According to their calculation, the Indo-Gangetic area temperature decrease. Heat index and wet-bulb temperature increase due to irrigation (figure 8 d-f). They concluded that the decline in dry heat and increase in moist heat in Indo-Gangetic Plain can be attributed to the combination of large-scale climate warming and the localized effect of irrigation.

1.3 Scientific questions and hypotheses

According to the discussion above, we can conclude some important characteristics of T and Tw affected by irrigation. First of all, irrigation is a cooling effect on T. Also, it can moisturize the surface air by PBL collapse and the specific humidity goes up. Thus, irrigation on wet-bulb temperature is a competing effect. Irrigation is an increasing factor in Tw from April to May (Vimal et al. (2020)). However, what scenario can cause

the moistening or cooling effect to dominate? Will irrigation worsen or alleviate the extreme on T_w ?



To understand the characteristic of T_w , we take figure in Roland et al. (2011) as a reference (figure 9). We can see that when RH is low and T is high, the T_w curve is more horizontal than in other conditions. That is to say, when increasing RH, it is easier to increase T_w . Because of this characteristic, the cooling effect is not easy to apply on T_w . On the other hand, if RH is high, the T_w curve is more vertical, so the moistening effect is not apparent as the cooling effect.

In a nutshell, our hypotheses are as below. If background RH is low and temperature is high, the irrigation moistening effect dominates. However, if background RH is high, the irrigation cooling effect dominates.

Chapter 2. Data of the coupled climate model and method



2.1 Data

We use the same data as used in Wim et al. (2020), which is a fully coupled CESM model (version 1.2). Also, version 4.0 of the Community Land Model (CLM) represents the land surface in CESM1 (Wim et al. (2020)). Vegetation state and soil moisture content in one soil column for irrigated crops calculate the irrigation module. In CLM 4.0, greenhouse gas concentrations and satellite-derived vegetation phenology are considered. The resolution of all simulations is $0.9^\circ \times 1.25^\circ$. Here, we use three main variables. Daily maximum temperature on reference height (T_{ref}), daily mean relative humidity on reference height (RH_{ref}), and daily mean surface pressure to calculate the specific humidity (or mixing ratio) and wet-bulb temperature. In Community Atmosphere Model (CAM), the reference height is 2m height. Note that the 2m height temperature and specific humidity (or relative humidity) in this model are calculated by the Monin-Obukhov similarity theory (David et al. 2019). The theory indicates that the temperature and humidity profiles in the boundary layer are determined by the Monin-Obukhov length (L) which is related to the stability of the atmosphere and the shear wind. In specific, the 2m height temperature is related to the gradient of potential



temperature between the atmosphere and surface and the Monin-Obukhov length (L)

(David et al. 2019).

The reason why we use model data is that only the model can isolate the single process, while observation data is a lumped signal.

The transfer of T , RH , and P to T_w is as below:

(1) Use the c-c equation to get saturated vapor pressure.

$$e_s(T) = e_{s0} \exp\left(-\frac{L_v}{R_v}\left(\frac{1}{T} - \frac{1}{T_0}\right)\right) \quad (1)$$

(2) Use the definition of relative humidity.

$$e = RH * e_s \quad (2)$$

(3) Use the definition of mixing ratio.

$$w = \frac{0.622e}{p - e} \quad (3)$$

(4) Calculate T_w using 15 iterations of bisection method.

$$T_w = T_i - \frac{L_v}{R_v}\left(\frac{0.622}{p} A \exp\left(-\frac{B}{T_w} - w\right)\right)$$



where A and B are constants.

2.2 Method

Here, following Wim et al. (2020), we use the linear regression technique to isolate an individual forcing from a lumped signal.

$$\Delta TXm = \beta_1 \times \Delta f_{irr} + \beta_2 \times lat. + \beta_3 \times lon. + \beta_4 \times elev. \quad (5)$$

Δf_{irr} represents the irrigation fraction difference between 1901-1930 and 1981-2010.

The longitude, latitude, and elevation terms represent other effects. The irrigation-induced temperature change in the pixel ΔTXm_{irr} can be obtained by taking out the coefficient of Δf_{irr} , which can be written as

$$\Delta TXm_{irr}(i) = \beta_1 \times \Delta f_{irr}(i). \quad (6)$$

We hypothesize that specific humidity and Tw may not depend on the locations. To optimize the regression process and not take other variables into our calculation, we need to investigate the CESM experimental simulations. Table 1 represents the CESM



productions.

Then, we can do some calculations between these four simulations. We assume the linear responses when we decompose the irrigation and other effects for the multiple linear regressions. The non-linear effect may exist in these analyses, but we make the linear assumption to get the first-order characteristic of irrigation. The first one is control minus 20cc, which represents the other forcing change between 1901-1930 and 1981-2010. The second one is irr minus 20cirr, which explains the other forcing plus irrigation effect. These two results could be used to distinguish the lumped signal.

By doing so, we propose a new concept of regression technique as below:

$$\Delta TXm_{irr-20cirr} = \beta_1 \Delta f_{irr} + \beta_2 \Delta TXm_{ctl-20cc} + a_1 \quad (7)$$

$$\Delta qXm_{irr-20cirr} = \beta_1 \Delta f_{irr} + \beta_2 \Delta qXm_{ctl-20cc} + a_2 \quad (8)$$

$$\Delta TwXm_{irr-20cirr} = \beta_1 \Delta f_{irr} + \beta_2 \Delta TwXm_{ctl-20cc} + a_3 \quad (9)$$

where q represents specific humidity. The terms on the left-hand side are signals with irrigation and other forcings at the same time. $\beta_1 \Delta f_{irr}$ is the irrigation effect and β_2

terms are other forcings. That is to say, we can distinguish a lumped signal and use the simulation without taking other variables into our calculation.





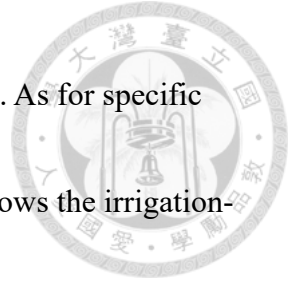
Chapter 3. Results of coupled climate model

Between 1901-1930 and 1981-2010, the irrigation fraction expanded in the Central USA, Europe, South Asia, and North China. Figure 10 shows that Indo-Gangetic Plain expanded up to 50-60 percent of irrigation, and North China expanded by 30-50 percent. Here, we divide these places as global land, Central USA (42.5°W-111.25°W, 31.57°N-42.88°N), North China (108.75°E-121.25°E, 27.80°N-41.00°N), Europe (0°E-32.5°E, 35.34°N-56.07°N), and South Asia (68.75°E-90°E, 5.18°N-32.51°N).

Figure 11 shows when irrigation expands, ΔTXm decreases in all regions. If the change in irrigated fraction equals 0, there is no irrigation expansion. We can see that ΔTXm is about 0.5K which is the anthropogenic warming signal. If we focus on the irrigation-induced effect (second column), ΔTXm_{irr} decreases because of negative β_1 .

3.1 Global land

Figure 12 demonstrates the same idea as figure 11 except for the definition of ΔTXm . Here, we capture the change in average daily maximum wet-bulb temperature during the hottest month of the year, named $\Delta TwXm$. Then, we get the dry-bulb temperature and specific humidity at the time of $TwXm$. In the first row of figure 12,



global land T_w increases by 0.5K. T goes down as irrigation expands. As for specific humidity, it increases by 0.0005 to 0.001 (kg/kg). The second row shows the irrigation-induced effect. We can see that when Δf_{irr} equals 0.5, anomalous temperature decreases to -0.5K. As for specific humidity, Δf_{irr} goes up and Δq also increases because of irrigation replenishing water into the soil and evaporating. The slope is about $5 \times 10^{-4}/0.5$ ($\Delta q/\Delta f_{irr}$). In this scenario, the T_w increases because the moistening effect dominates.

To discern whether the moistening effect dominates, we introduce the differentiating of the definition of T_w . Here, we assume that constant P is 1013 (hPa) and 300 (K) into T_w in equation (13):

(1) The definition of T_w .

$$T_w = T - \frac{L_v}{R_v} \left(\frac{0.622}{p} A \exp \left(-\frac{B}{T_w} - w \right) \right) \quad (10)$$

(2) Differentiate it in both side.

$$d(T_w) = d \left[T - \frac{L_v}{R_v} \left(\frac{0.622}{p} A \exp \left(-\frac{B}{T_w} - w \right) \right) \right] \quad (11)$$



(3) Use the chain rule to deal with the exponential term.

$$d(T_w) = dT - \frac{L_v}{R_v} \left(\frac{0.622}{p} A \exp\left(-\frac{B}{T_w} - w\right) \right) \left(\frac{B}{T_w^2} dT_w - dw \right) \quad (12)$$

(4) Distinguish each variable.

$$\left(1 + \frac{L_v}{R_v} \frac{0.622}{p} A \exp\left(-\frac{B}{T_w} - w\right) \frac{B}{T_w^2} \right) dT_w = dT + \frac{L_v}{R_v} dw \quad (13)$$

The left-hand side of the factor is about 8.07. The error for the pressure is -0.97% when decreasing 10hPa. It is so small that the assumption of constant pressure is reasonable.

As for all forcing, dw is about 0.001 (kg/kg). Then, when plugging these numbers into equation (13) above then we get:

$$dT_w = 0.12dT + 0.67 \cong 0.67 \sim 0.7 \quad (14)$$

which is similar to the T_w in all forcing plots. Note that the effect of specific humidity change on T_w is larger than the temperature change. The same concept can be applied in

irrigation induced plots to examine which one dominates when $\Delta f_{irr} = 0.5$, plug

$dw = 5 \times 10^{-4}$ given by figure 12e. Then we have:

$$dT_w = 0.12dT + 0.335.$$



(15)

The dT term cannot cancel out the dw term, so the moistening dominates and T_w

increases about 0.3 (K) at $\Delta f_{irr} = 0.5$.

3.2 Central USA

Figure 13 shows the change of T_w in the Central USA. In the first row, T_w increases 0.5 (K) in all Δf_{irr} when the specific humidity increases as a constant and dominates although dry-bulb temperature decreases about 0.5 (K) in 50% of irrigation expansion. In the second row, we found that T_w is canceled out by the decreasing temperature and increasing specific humidity. The main reason comes from the irrigation fraction induced specific humidity change is lower than global land.

We can plot a diagram to discern whether dT or dw is dominated. Assuming that constant P is 1013 (hPa), figure 14 shows the equivalent dry-bulb temperature effect on T_w when the mixing ratio changes. That is to say, if the mixing ratio increases 0.2×10^{-3} (kg/kg), it equals to an increase of 1 (K) of dry-blub temperature. If we need to cancel out the moistening effect, the dry-blub temperature must decrease by 1



(K) so that the right-hand side of equation (13) equals zero. Another aspect of this picture tells us how to discern which one is the dominant factor. The area above the blue line means the temperature effect is over the moistening effect. Thus, if we want to get the result that T_w is dominated by the cooling effect, the moistening of dw must as small as possible. This can make the cooling signal not be canceled out by the moistening effect.

3.3 North China

In the first row of figure 15, we can see the same effect as above. The specific humidity change is about 10^{-3} (kg/kg), so the T_w is dominated by the moistening effect although the temperature decreases when irrigated fraction goes up. On the other hand, the specific humidity induced by irrigation is small so the T_w has the same trend as temperature. The specific humidity changes almost come from anthropogenic forcing, not from irrigation expansion. This may be due to the idea of the c-c equation. When anthropogenic forcing causes greenhouse gas emissions to increase, the temperature goes up. Therefore, the air parcel could hold more water vapor than before, which makes the specific humidity increase homogeneously.



3.4 Europe

Europe is a special case in these areas. In figure 16, we can find that the wet-bulb temperature increases a lot because of the large change in specific humidity. This change comes from irrigation induced effect; that is to say, adding water to soil is much more effective in evaporating into the atmosphere, which causes the rapid increase of specific humidity and decreases the temperature. The evaporation allows water vapor to take away the heat and increase the enthalpy of the near-surface.

3.5 South Asia

In South Asia, it is a good case to discuss the irrigation effect on heat waves because of the high temperature of the dry season and the wet season, from April to May and July to August, respectively. In addition, the irrigation area in Indo-Gangetic Plain is also larger compared to other places. Therefore, we discuss this place more comprehensively to figure out the effect of irrigation on wet-bulb temperature.

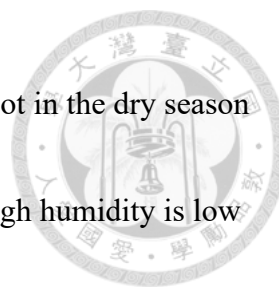
First of all, we do the same analysis on the change in the wet seasons. In the nutshell, during the wet seasons, the wet-bulb temperature increases by 0.5 (K) in figure 17c because of the change in specific humidity. But why the specific humidity doesn't



go up when the irrigation fraction increases in figure 17b?

To figure out the reason, we distinguish the irrigation effect and other effects in the map. Figure 18 shows the specific humidity change induced by other forcings. The contour represents the irrigation fraction which illustrates that Northeast India is a highly irrigated area. Interestingly, the specific humidity decreases in high and increases in low irrigated areas. The mechanism comes from the irrigation cooling effect. When the irrigation makes the surface temperature goes down, that means the air parcel cannot hold as much water vapor according to the c-c equation. On the other hand, global warming makes the temperature in other places rise. In summer, the monsoon brings lots of moisture into India, so the higher temperature place can hold much more water vapor. Therefore, the increasing moisture from irrigation and the decreasing moisture from the cooling effect cancel out. That's why the specific humidity in figure 17b stays still as the irrigated fraction increases.

For the dry season in figure 19, we analyze the T_w change in South Asia from April to May. We can see that the T_w change over 1 (K) as the irrigated change fraction equals 0.3, which is much higher than the wet season. The reason also comes from the increased specific humidity, which almost results from the irrigation. In this part, it is



important to understand that the range of the humidity can change a lot in the dry season and it is from the irrigation expansion. On the other hand, the 10m high humidity is low so the gradient of humidity increases, which makes the evaporation work effectively.

Although it effectively cools down the surface temperature, the cooling effect is little compared to the moistening effect. Therefore, the heat wave in the dry season might be dangerous for humans because the air parcel can have much more water vapor and make the atmosphere humid leading to a higher T_w .

Figure 20 shows the irrigation effect of one month's average in South Asia. The irrigation effect is the simulation from irr minus control in table 1. The criteria is RH lower than one standard deviation. Note that the red dots represent temperature change is the dominant factor. That is to say, the absolute value of the temperature difference is larger than the mixing ratio.

According to our calculation, when the mixing ratio change is small compared to the temperature change, the T_w change and T change are linear. The regression slope of the red dots is 0.20 which is close to the theoretical value of 0.125. On the other hand, if the mixing ratio change is over about 0.0003 (kg/kg), the moistening effect dominates the region. This means the wet-bulb temperature change is positive no matter how the



dry-bulb temperature change is induced by the irrigation effect, so most of the black dots are situated in the first and second quadrants in the left diagram due to the moistening effect. Note that the red-to-black ratio is low so the possibility of temperature change dominating in the dry condition is low. In addition, this is evidence that the T_w is more sensitive to mixing ratio change.

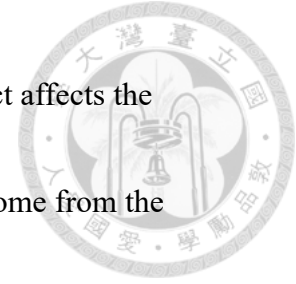
Same as above, the red region represents the temperature change dominating the area over the wet conditions (Figure 21). Comparing figure 20 and figure 21, the red dots of dry-bulb temperature in dry condition skew to the negative value. However, in wet conditions, the red dots of dry-bulb temperature do not skew to the negative value, which means the temperature cooling effect does not exist in this scenario. This phenomenon can be seen in figure 22a which is the probability density function of temperature change. The definition of dry and wet conditions is the same as in figures 20 and 21. To confirm the significance, we set the hypothesis as below:

$$H_0: \mu_{dry} \geq 0$$

$$H_1: \mu_{dry} < 0$$

(16)

The one-tail test tells us that the z-value is low enough to reject the null hypothesis, and



the p-value is lower than 0.01. Therefore, the irrigation cooling effect affects the temperature in dry conditions significantly. The mechanism might come from the gradient of humidity between the soil and the atmosphere increasing so evaporation works effectively compared to wet conditions.

To find the possibility of the temperature change dominating region, we do the possibility density function of wet and dry conditions and the result is shown in figure 22b. First of all, the probability of wet conditions of mixing ratio changes close to 0 (kg/kg) is higher than in dry conditions. Also, we do the one-tailed z-test to verify the red line skews to the positive value. The hypothesis is as below:

$$H_0: \mu_{dry} \leq \mu_{wet}$$

$$H_1: \mu_{dry} > \mu_{wet}$$

(17)

The z-value equals 5.0661 and the p-value is lower than 0.01, which means we have 99% confidence to reject the null hypothesis and the mean value of mixing ratio change is significantly skewed to a positive value.

In addition, the variance is also important when we investigate the moistening effect. Here, we do the one-tailed F-test to verify whether the variance of dry conditions

is larger than wet conditions. The hypothesis is as below:

$$H_0: \sigma_{dry}^2 \leq \sigma_{wet}^2$$

$$H_1: \sigma_{dry}^2 > \sigma_{wet}^2.$$

(18)

The F value is 6.9501 and the critical value is 1.0956, which means we have 99% of confidence in rejecting the null hypothesis. In this analysis, we can conclude that the distribution of dry conditions is wider than wet conditions. The probability of suffering from an extreme event is higher than in wet conditions because of the skewed and wide distribution. Therefore, the ratio of dots on the left-hand side of figure 20 in the first and second quadrants to the third and fourth quadrants is larger than that in figure 21. Also, some wet-bulb changes can reach up to 6 (K) in figure 20, which results from the extreme value of the change of mixing ratio.

As the discussion above, it is interesting to investigate the mechanism of evaporation influenced by the gradient of soil and air moisture. Here, we explore the difference in latent heat flux change. As shown in figure 22c, the dry condition curve skews to the positive value. This means the net effect of irrigation for dry conditions can bring more evaporation, especially from April to May (as appendix A2). Note that the



appendix figures point out the dry seasons and wet seasons in South Asia. The number in the parentheses denotes the number of dry or wet events from 1981 to 2010. From



April to May, the climate is hot and dry, which means the background relative humidity is low. If we add water to the soil, the gradient of moisture goes up and makes evaporation effective. On the other hand, we find that there is no apparent difference in other seasons. In summary, the cooling effect of irrigation on dry-bulb temperature is sensitive due to the effective evaporation. This is an important conclusion to discuss the characteristic of temperature in each condition.



Chapter 4. Results of the offline land surface model

4.1 Data

In this chapter, we use version 5.0 of the Community Land Model (CLM) to represent the land surface in CESM and apply offline simulation which spins up in 1901 for 5 years and duration between 1901 to 2014 (David et al. 2019). The resolution of all simulations is $0.9^{\circ} \times 1.25^{\circ}$. Here, to demonstrate the mechanism between evaporation and irrigation, we use seven variables, which are ground temperature (T_g), 2m high temperature (T_{2m}), 2m high specific humidity (q_{2m}), atmospheric specific humidity (QBOT), sensible heat flux (SH), latent heat flux (LH), and wind speed (U). The reason why we use the offline model is that it is clearer to know the mechanism of evaporation. Compared to coupled model, the reaction on the ground would not influence back to the atmosphere, so the change on the ground is simple to learn the pure process.

In the offline model, the irrigation is made once per day at 6 AM local time (David et al. 2019). The model would calculate each pixel whether the irrigation moisture is over the threshold. If it is over the threshold, the model keeps the pixel in the same soil moisture. However, if the pixel's moisture is under the threshold, the model irrigates to the available moisture (David et al. 2019).

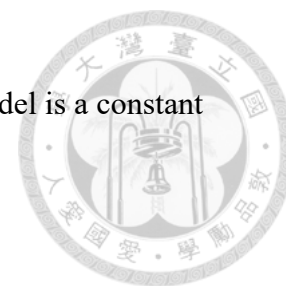
4.2 Comparison between offline and coupled model



Figure 23 shows the difference between the offline and coupled models. First of all, the red line represents the coupled model temperature on the ground and the black (dash) line represents the ground (2m high) temperature. The red line has higher annual variability compared to the black line. This comes from the characteristic of the offline model which is calculated by bounded atmospheric information. That is to say, the irrigation and control run have the same forcing in the atmosphere to calculate the variables on the ground. However, the coupled model means that the surface information can influence the atmosphere by land-atmosphere interactions, so the atmospheric information is not the same in each time step.

Also, the change of the black dash line is not as large as the solid line. This is because the 2m high temperature is interpolated by the surface and bounded atmosphere (David et al. 2019). Therefore, it includes the information of higher atmosphere which is the same in control and irrigation run. Finally, during the daytime, evaporation works more compared to night, so both offline and coupled models have a larger decrease in temperature during the daytime. Again, in the CLM model, the 2m high temperature and specific humidity are calculated based on the similarity theory assuming that the surface

heat between the surface and the bottom layer of the atmosphere model is a constant with height (David et al. 2019).

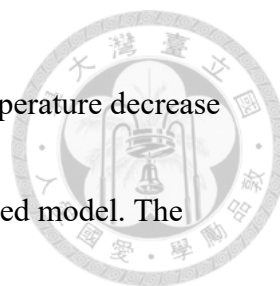


4.3 The scatter plot in South Asia

Here, we plot the scatter plot as same in section 3.5. In figure 24 and 25, the absolute value of the difference in mixing ratio is smaller than those in figure 20 and 21, which comes from the same reason as section 4.2. The bounded atmosphere makes the 2m high mixing ratio change not as large as the coupled model. In addition, because the surface information cannot be a forcing to the atmosphere, most of the mixing ratio dots move to the positive axis when we turn on the irrigation due to the moisture going to the atmosphere and not dissipated by the coupling process.

Overall, we can get the same result that the drier season in figure 25 makes evaporation work efficiently to increase the mixing ratio and decrease the temperature at the same time. However, most of the dots are black, which means the mixing ratio change is a dominant factor as far as wet-bulb temperature is concerned.

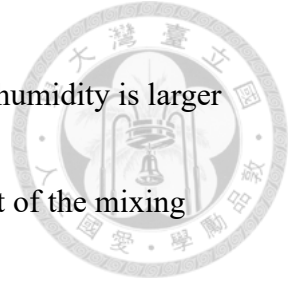
Figures 26a and 26b are the conclusions above. The temperature and mixing ratio change are narrowed to zero and shifted to the positive value compared to the coupled



model. Also, dry conditions have a larger tail of moisturized and temperature decrease compared to wet conditions. Here, we get similar results as the coupled model. The evaporation works efficiently in dry conditions so that the possibility density distribution curve shifts to moistening and cooling values. However, evaporation doesn't work efficiently in wet conditions, so the mean value is close to zero and symmetry to zero value.

4.4 The diurnal difference in the dry and wet seasons (South Asia)

Figure 27 shows the difference in temperature, wet-bulb temperature, and mixing ratio in the dry season, respectively. On dry season days, the gradient of humidity between irrigated surfaces and the atmosphere is large. Therefore, evaporation works more effectively than the night and wet seasons. However, according to equation (13), the moistening effect is much larger than the temperature decrease. Thus, the wet-bulb temperature curve is similar to the mixing ratio change. Specifically, the curve of mixing ratio change increased from 1906 to 2010 because the irrigation amount in South Asia also increases and makes the evaporation go larger. During the nighttime, the temperature decreases because of sunsets. Besides, the moisture in the atmosphere

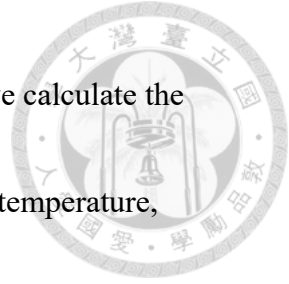


goes higher from evaporation in the daytime. Therefore, the relative humidity is larger at night than at daytime. Evaporation is less due to the lower gradient of the mixing ratio between the surface and atmosphere and solar radiation. Thus, the red curve in figure 27 has the same trend as the blue curve, but the absolute values are lower.

Figure 28 shows the difference in temperature, wet-bulb temperature, and the mixing ratio in wet seasons, respectively. In these figures, the daytime and nighttime are similar. This is because the background atmosphere is wet and the gradient between the surface and atmosphere is small both day and night. Therefore, the wet-bulb temperature doesn't increase as large as in dry seasons but still has the same trend.

4.5 The yearly trend of wet-bulb temperature in South Asia and North China

In this section, we explore six variables to deeply understand the mechanism of irrigation moistening by comparing two different regions, South Asia and North China. Figure 29 shows the difference in variables due to irrigation. Figure 29d illustrates the irrigation amount increase over time. This is due to the increasing population and the food demand getting higher, particularly after the 1950s (Siebert et al. 2015, Guo et al. 2022). Because of these higher amounts of water in the soil, the specific humidity near



the surface gets higher, making evaporation efficient. Accordingly, we calculate the correlation coefficient of irrigation amount to temperature, wet-bulb temperature, mixing ratio, and latent heat flux. The coefficients are -0.993, 0.994, 0.997, and 0.991, respectively. Therefore, the relations between these variables are highly correlated.

To analyze what makes the evaporation work, we investigate the bulk formula which is the concept of the mixture in the boundary layer (Lawrence et al. 2019) as below:

(1) The definition of the bulk formula:

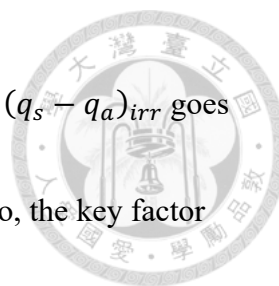
$$LH = \rho L_E C_L U_{10} (q_s - q_a) \quad (19)$$

(2) Differentiate it on both sides:

$$dLH \propto U_{10} d(q_s - q_a). \quad (20)$$

Therefore, the difference in latent heat flux between the two models is in proportion to the specific humidity difference. Figure 29f shows the decomposition of latent heat flux.

The main reason that causes the evaporation to work is the difference of specific humidity in the atmosphere and surface, here we call $(q_s - q_a)_{sub}$ afterward and the



subscript means the simulation model. When irrigation turns on, the $(q_s - q_a)_{irr}$ goes higher because the specific humidity gets larger near the surface. Also, the key factor

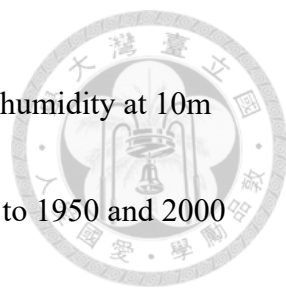
$d(q_s - q_a)$ can be written as:

$$d(q_s - q_a) = (q_s - q_a)_{irr} - (q_s - q_a)_{ctl} = (q_s)_{irr} - (q_s)_{ctl} \quad (21)$$

Note that this is a bounded model, so the specific humidity of the atmosphere is the same in both models. Note that figure 29f is similar to figure 29e but not the same. This comes from the coefficient ahead in equation (19) is not the same when the model does the irrigation.

In plain language, the mechanism is that evaporation makes the surface moisturize, which causes evaporation to work efficiently. This gives rise to latent heat flux and the mixing ratio goes high. Also, the temperature goes down due to the cooling effect. The result of wet-bulb temperature obeys the mixing ratio curve because the moistening effect is the key faction to dominate.

Figure 30 is the profile of North China, the irrigation amount is less than South Asia by one order. Thus, the evaporation-related variables change less. However, although the irrigation amount increases over time, latent heat flux decreases between



1920 to 1950 and 2000 to 2010. Figures 31a and b show the specific humidity at 10m and 2m high. It grows about 10^{-3} (kg/kg) and 10^{-4} (kg/kg) from 1920 to 1950 and 2000 to 2010. That is, the background atmosphere is moisturized. According to our discussion above, the evaporation is less because of the specific humidity difference in the two models, that is, $(q_s)_{irr}$ minus $(q_s)_{ctl}$, gets lower. Therefore, the related variables (i.e. wet-bulb temperature, mixing ratio, etc.) have the same trend as latent heat flux although the irrigation amount remains nearly the same.

Also, we find that the irrigation amount increases rapidly from 1950 to 1960. This might come from two factors at the same time. The first one is the green revolution which is the food demand from the increasing population. The second one is the background atmosphere becomes dry. Figure 31a shows the decreasing specific humidity in the upper layer from 1950 to 1960. That is to say, the model is forced to irrigate this region due to the increasing irrigation fraction and the dry climate. Therefore, the latent heat flux increases rapidly because the specific humidity near the surface gets much higher compared to the control simulation. Therefore, the mixing ratio and wet-bulb temperature increase a lot over this period.

Chapter 5. Discussion



Here, we revisit our hypothesis. If the background RH is low, the irrigation moistening effect would dominate. Due to the higher standard deviation of the mixing ratio changing, the T_w might have a higher chance of extremes. On the other hand, if the background RH is high, the evaporation is less from the lower water gradient. Therefore, there is no apparent cooling or moistening effect to alter the T_w .


Some may argue that the T_w is so low in the dry condition that we should not concern about heat stress here. We analyze the T_w mean and extreme value shown in figure 32. Figures 32a and 32b illustrate the T_w average in dry and wet seasons in India, respectively. Indeed, the heating center (figure 32e) is located in the apparently low T_w area. However, we consider the most dangerous place to be located in the transient zone (at the edge of the heating center) where the T_w is not low but the evaporation still works. In this area, the moistening effect still exists to increase the T_w . On the other hand, figure 32g shows the maximum T_w difference (irrigation run minus control run), the edge of the heating center makes the extreme value in figure 32c increase nearly the same as the T_w maximum in the wet season in figure 32d. Also, in figures 32f and 32h, the difference between control and irrigation run in the wet season is small compared to



the dry condition. Therefore, this is evidence that the moist heat stress is a concern when it comes to the mean and extreme value in the dry condition in the Indo-Gangetic Plain.

In our simulations, the irrigation amount comes from the threshold of soil moisture. If the soil moisture is lower than the threshold, the model irrigates the pixel to the available amount which means the soil cannot hold any more water. Jha et al. (2022) argue that the irrigation amount in the dry season in India is overestimated by the CLM model because of the policy of the Indian government to preserve the water. They use census-based data from satellite observation and find that the heat stress is overestimated by 4.9 times in the model. In our perspective, we use the CLM model to know that evaporation is a key factor controlling wet-bulb temperature and heat stress. Irrigation can really make the regional wet-bulb temperature increase due to the higher humidity. However, after exploring its mechanism, we could combine the census-based irrigation amount to analyze the effect of irrigation in the real world. This can be investigated in the future so that the climate in the irrigated world would not be overestimated.

In addition, several studies estimate that irrigation inputs more water vapor into the



atmosphere, which makes the surface warming temperature be overlooked (Kenny & Hodzic, 2019). Li et al. (2022) used two different assumptions to simulate with or without global irrigation. Their results show that the temperature in both day and night time drops due to irrigation in the first case. This comes from the reduction of shortwave radiation by the increasing mid-level cloud, which is consistent with our simulation and assumption. However, they argue that moisture in the atmosphere is a greenhouse gas that makes the reflected longwave radiation increase and makes the surface temperature goes up at the same time. From our viewpoint, this is truly a new discovery that is different from most previous research. But for the wet-bulb temperature, although the dry-bulb temperature goes up, the wet-bulb temperature would not change a lot because the temperature effect is not large.

We consider the CTX method (Perkin and Alexander, 2013) to be a way to measure the frequency and strength of heat waves when it comes to moist heat stress. They define the threshold of each day by taking the 90th percentile of T_{\max} using a 15-day running window for 46 years. The reason why they use the running window is that the climate signal may advance or delay on some days. By doing so, a window average is a better index to represent a climate condition. CTX gives us a benchmark to analyze the

characteristic of heat waves and this can be applied to how the T_w could be affected extremely under the moistening effect.



For the farmers in the Indo-Gangetic Plain, the seasonal to annual projection is very important to avoid exposure to heat stress. Climate Services Toolbox (CSTools) is a useful tool based on R packages to visualize climate information (Núria et al., 2022). They use state-of-art methods to downscale and plot the probability density function to present the data. By using this tool, we can evaluate the moistening effect on T_w to alert the farmer not to expose to the heat condition with higher resolution.

Ultimately, our results are consistent with Guo et al. (2022) using ERA-5 reanalysis data. They argue that the ERA-5 data is assimilated with observed datasets every 6 hours so it is reliable data. We consider that the ERA-5 data is similar to our offline control simulation. They explore the wet-bulb globe temperature to demonstrate the heat stress due to shortwave radiation. This can be our future work to investigate the wind speed and shortwave radiation in the CLM model combining census-based irrigation data. By doing so, we can separate the irrigation effect from the lumped signal and get more detailed information about heat stress and comfort.

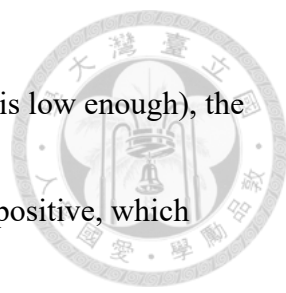
Chapter 6. Conclusions



In this study, we use NCAR CESM and CLM models to assess the near surface climate changes. The impact of irrigation on wet-bulb temperature from cooling and moistening effects is explored. We use the technique of linear regression to distinguish the effect of global warming and irrigation. Overall, irrigation is a cooling effect in the area we choose. As for wet-bulb temperature, there are two competing effects. The moistening and the irrigation cooling effects can increase and decrease the wet-bulb temperature, respectively. However, the background climate conditions could be a key factor in wet-bulb temperature change due to the amount of evaporation.

As shown in figure 33, if the background relative humidity is wet, there are two scenarios. (a) If the wet-bulb temperature is controlled by dry-bulb temperature, the irrigation cooling effect doesn't exist apparently because the mean of latent heat flux change is nearly zero. (b) If it is controlled by the mixing ratio, the wet-bulb temperature would be divided into two parts. As the mixing ratio increases, the wet-bulb temperature also goes up, and vice versa.

From our simulations, if the background is dry, the wet-bulb temperature is more likely controlled by the mixing ratio change. However, if the wet-bulb temperature is



still controlled by the dry-bulb temperature (the mixing ratio change is low enough), the irrigation cooling effect exists because the latent heat flux change is positive, which makes the wet-bulb temperature drop. On the other hand, if the wet-bulb temperature is controlled by the mixing ratio, the wet-bulb temperature is more likely to increase because the distribution of the mixing ratio change skews to a positive value and the standard deviation is larger than that in the wet condition.

In the nutshell, the cooling effect and moistening effect are not apparent due to the less evaporation in the wet condition. On the other hand, irrigation might worsen comfort in view of the wet-bulb temperature, which is consistent with the result of Mishra et al. (2020). Ultimately, the wet-bulb temperature is so sensitive to the mixing ratio change that it is a critical factor when we focus on comfort and moist heat stress.

Chapter 7. References



- [1] Chou, Chihchung, et al. "Irrigation-induced land–atmosphere feedbacks and their impacts on Indian summer monsoon." *Journal of Climate* 31.21 (2018): 8785-8801.
- [2] David M. Lawrence, Rosie A. Fisher, Charles D. Koven, Keith W. Oleson, Sean C. Swenson, Gordon Bonan, Nathan Collier, Bardan Ghimire, Leo van Kampenhout, Daniel Kennedy, Erik Kluzek, Peter J. Lawrence, Fang Li, Hongyi Li, Danica Lombardozzi, William J. Riley, William J. Sacks, Mingjie Shi, Mariana Vertenstein, William R. Wieder, Chonggang Xu, Ashehad A. Ali, Andrew M. Badger, Gautam Bisht, Michiel van den Broeke, Michael A. Brunke, Sean P. Burns, Jonathan Buzan, Martyn Clark, Anthony Craig, Kyla Dahlin, Beth Drewniak, Joshua B. Fisher, Mark Flanner, Andrew M. Fox, Pierre Gentine, Forrest Hoffman, Gretchen Keppel-Aleks, Ryan Knox, Sanjiv Kumar, Jan Lenaerts, L. Ruby Leung, William H. Lipscomb, Yaqiong Lu, Ashutosh Pandey, Jon D. Pelletier, Justin Perket, James T. Randerson, Daniel M. Ricciuto, Benjamin M. Sanderson, Andrew Slater, Zachary M. Subin, Jinyun Tang, R. Quinn Thomas, Maria Val Martin, Xubin Zeng, 2019: The Community Land Model version 5: Description of new features, benchmarking, and impact of forcing uncertainty. *Journal of Advances in Modeling Earth Systems*, 11, 4245-4287. <https://doi->

org.cuucar.idm.oclc.org/10.1029/2018MS001583.



[3] Dunne, John P., Ronald J. Stouffer, and Jasmin G. John. "Reductions in labour capacity from heat stress under climate warming." *Nature Climate Change* 3.6 (2013):

563-566.

[4] Guo, Qiang, et al. "Irrigated cropland expansion exacerbates the urban moist heat stress in northern India." *Environmental Research Letters* 17.5 (2022): 054013.

[5] Huachen Li, Min-Hui Lo, Donfryeol Ryu, Murray Peel, Yongqiang Zhang, Possible increase of air temperature by irrigation.

[6] Im, E.S., Pal, J.S. and Eltahir, E.A. Deadly Heat Waves Projected in the Densely Populated Agricultural Regions of South Asia. *Science Advances*, 3, No. 8. (2017).

[7] Jha, R., Mondal, A., Devanand, A., Roxy, M. K., & Ghosh, S. (2022). Limited influence of irrigation on pre-monsoon heat stress in the Indo-Gangetic Plain. *Nature communications*, 13(1), 1-10.

[8] Kang, Suchul, and Elfatih AB Eltahir. "North China Plain threatened by deadly heatwaves due to climate change and irrigation." *Nature communications* 9.1 (2018): 1-9.

[9] Kennedy, Ivan, and Migdat Hodzic. "Testing the hypothesis that variations in



atmospheric water vapour are the main cause of fluctuations in global temperature." *Periodicals of Engineering and Natural Sciences (PEN)* 7.2 (2019): 870-880.

[10] Krakauer, Nir Y., Benjamin I. Cook, and Michael J. Puma. "Effect of irrigation on humid heat extremes." *Environmental Research Letters* 15.9 (2020): 094010.

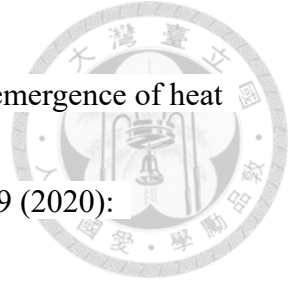
[11] Lawrence, David M., et al. "The Community Land Model version 5: Description of new features, benchmarking, and impact of forcing uncertainty." *Journal of Advances in Modeling Earth Systems* 11.12 (2019): 4245-4287.

[12] McNab, Brian Keith. *The physiological ecology of vertebrates: a view from energetics*. Cornell University Press, 2002.

[13] Mishra, V., Ambika, A.K., Asoka, A. *et al.* Moist heat stress extremes in India enhanced by irrigation. *Nat. Geosci.* **13**, 722–728 (2020).

[14] Pérez-Zanón, Núria, et al. "Climate Services Toolbox (CSTools) v4. 0: from climate forecasts to climate forecast information." *Geoscientific Model Development* 15.15 (2022): 6115-6142.

[15] Perkins, Sarah E., and Lisa V. Alexander. "On the measurement of heat waves." *Journal of climate* 26.13 (2013): 4500-4517.



[16] Raymond, Colin, Tom Matthews, and Radley M. Horton. "The emergence of heat and humidity too severe for human tolerance." *Science Advances* 6.19 (2020):

eaaw1838.

[17] Roland, S. Wet-Bulb Temperature from Relative Humidity and Air Temperature.

Science, **50**, 2267-2269. (2011).

[18] S. C. Sherwood, M. Huber, An adaptability limit to climate change due to heat

stress. *Proc. Natl. Acad. Sci. U.S.A.* 107, 9552–9555 (2010).

[19] Siebert S, Kummu M, Porkka M, Döll P, Ramankutty N and Scanlon B R 2015 A

global data set of the extent of irrigated land from 1900 to 2005 *Hydrol. Earth Syst. Sci.*

19 1521–45

[20] Thiery, W., Visser, A.J., Fischer, E.M. *et al.* Warming of hot extremes alleviated

by expanding irrigation. *Nat Commun* 11, 290 (2020).

[21] Vicedo-Cabrera, A.M., Scovronick, N., Sera, F. *et al.* The burden of heat-related

mortality attributable to recent human-induced climate change. *Nat. Clim.*

Chang. 11, 492–500 (2021).

[22] Wada, Yoshihide, et al. "Human water consumption intensifies hydrological drought worldwide." *Environmental Research Letters* 8.3 (2013): 034036.





	Time series	Natural forcing	Irrigation effect	Other forcing
20cc	1901-1930	Yes	No	No
20cirr	1901-1930	Yes	Yes	No
Control	1981-2010	Yes	No	Yes
Irr	1981-2010	Yes	Yes	Yes

Table 1. CESM simulation production.

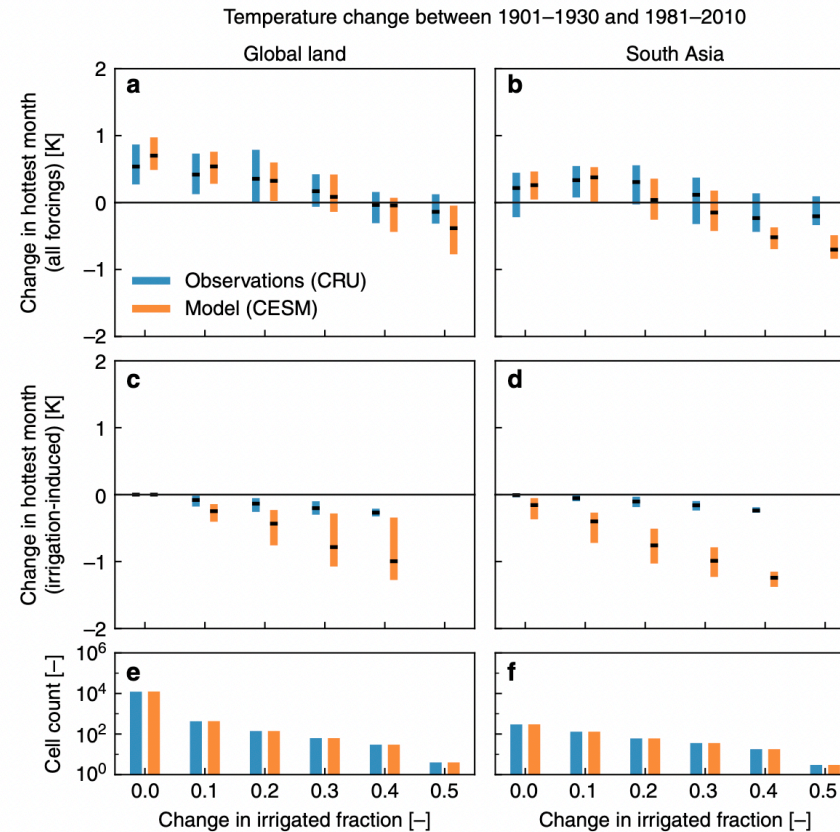


Figure 1. Observed warming rates affected by irrigation. Boxplots of the total (ΔTX_m , a, b) and irrigation-induced ($\Delta TX_{m_{irr}}$, c, d) change in average daily maximum temperature during the hottest month of the year for global land (a, c) and South Asia (b, d) between 1901 and 1930 and 1981 and 2010. This figure and legend are taken from Wim et al. (2020) figure 1.

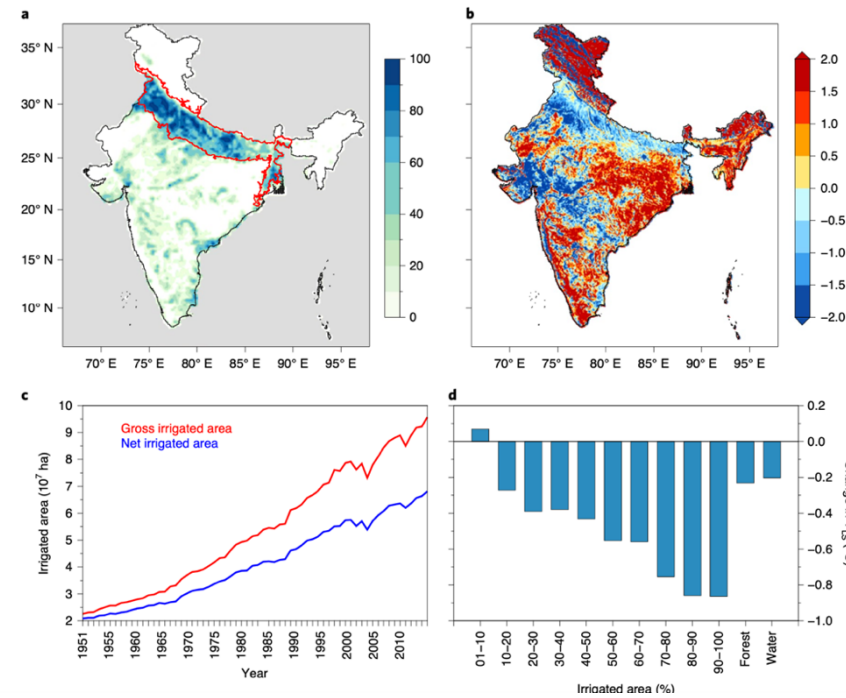


Figure 2. Irrigation driven cooling in the Indo-Gangetic Plain. **a**, Irrigated area (%) in India (data from the Food and Agriculture Organization). **b**, Changes in mean annual T_{LS} (°C) from the National Oceanic and Atmospheric Administration’s AVHRR (Advanced Very High Resolution Radiometer) for the period 1982–2015. **c**, Increase in gross and net irrigated area during 1951–2015 in India. **d**, Changes in T_{LS} for irrigated and non-irrigated regions in the Indo-Gangetic Plain. The area in the region outlined in red in **a** shows the highly irrigated region of the Indo-Gangetic Plain. The changes in **b** and **d** were estimated using a non-parametric mann–Kendall test and Sen’s slope method. This figure and legend are taken from Vimal et al. (2020) figure 1.

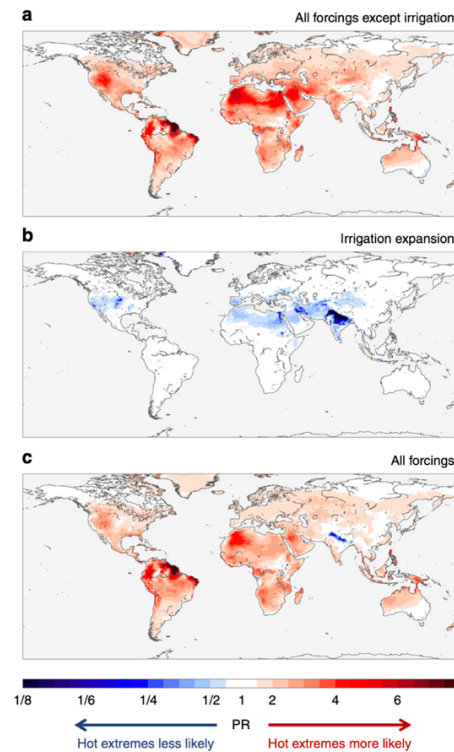


Figure 3. Change in probability of hot extremes from expanding irrigation and other forcings. Ensemble-mean likelihood of exceeding 99th percentile of daytime temperature (TX) as simulated by CESM, considering all forcings except irrigation (a), irrigation expansion only (b), and all forcings including irrigation expansion (c). Probability ratios (PRs) are shown for the present-day (1981–2010) relative to the early 20th century reference period (1901–1930), except for b where the reference is a counter-factual present-day world without irrigation. This figure and legend are taken from Wim et al. (2020) figure 2.

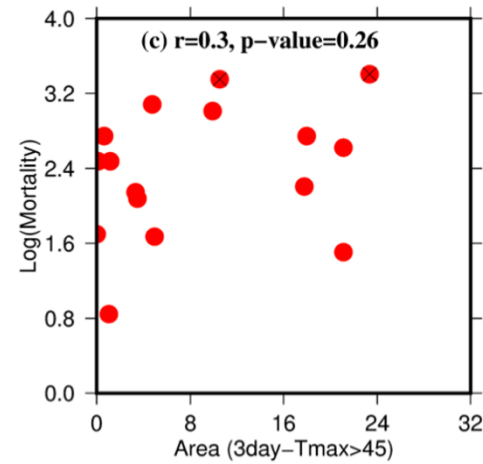
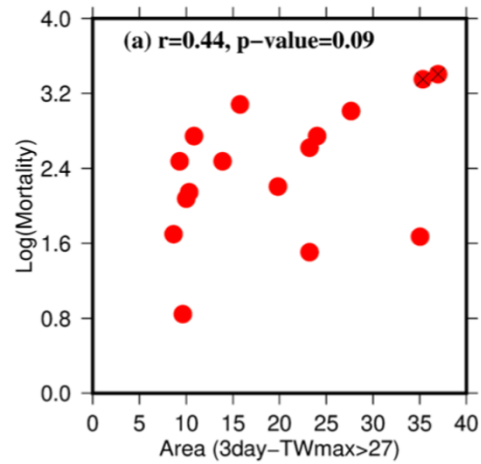


Figure 4. (a) Relationship between human mortality and area affected by extreme dry and moist heat stress (%) in India with 3-day maximum T_w greater than 27 during the heatwave. (c) same as (a) but for 3-day maximum T_2 greater than 45. Mortality data was obtained from EM-DAT (<https://www.emdat.be/>) for the 1979-2016 period. This figure and legend are taken from Vimal et al. (2020) figure S6.

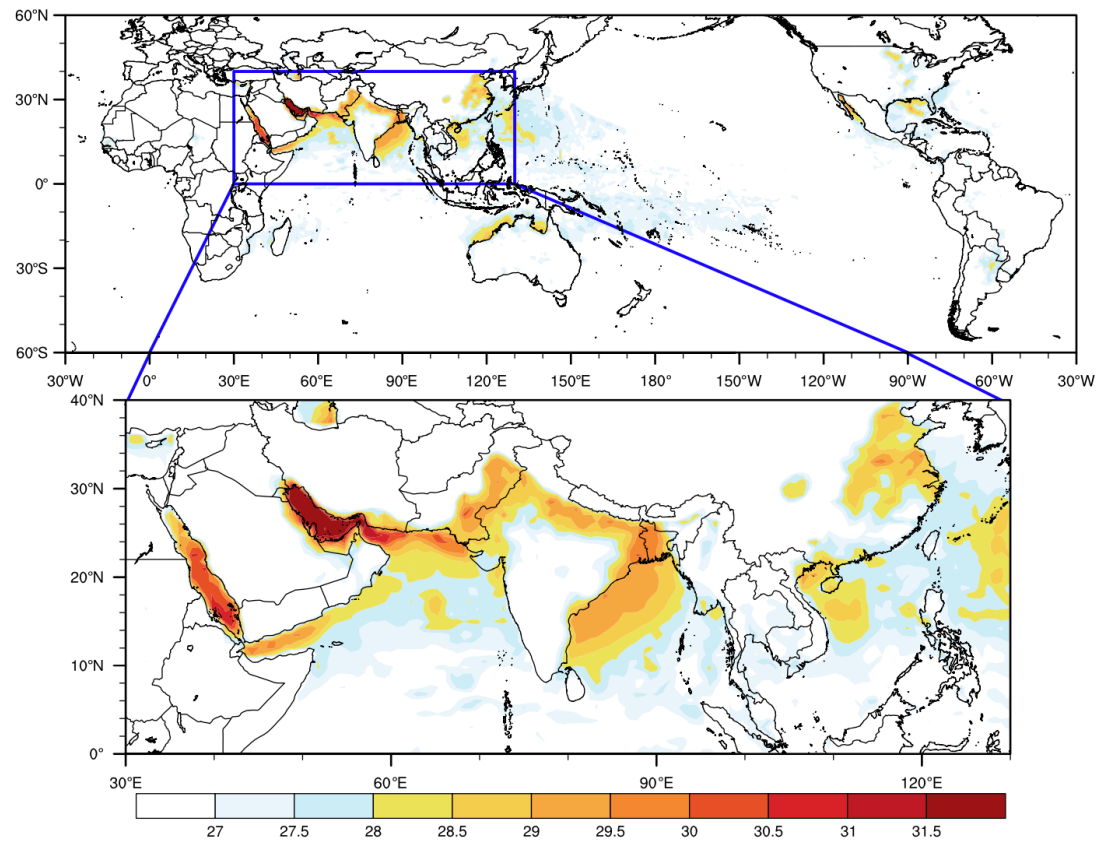


Figure 5. Spatial distribution of highest daily maximum wet-bulb temperature in modern record (1979-2015). Global distribution of $T_{w_{max}}$ is computed using ERA-Interim 3-hourly data with $0.75^\circ \times 0.75^\circ$ horizontal resolution. $T_{w_{max}}$ values below 27°C are not shown. This figure and legend are taken from Im et al. (2017) figure 1.

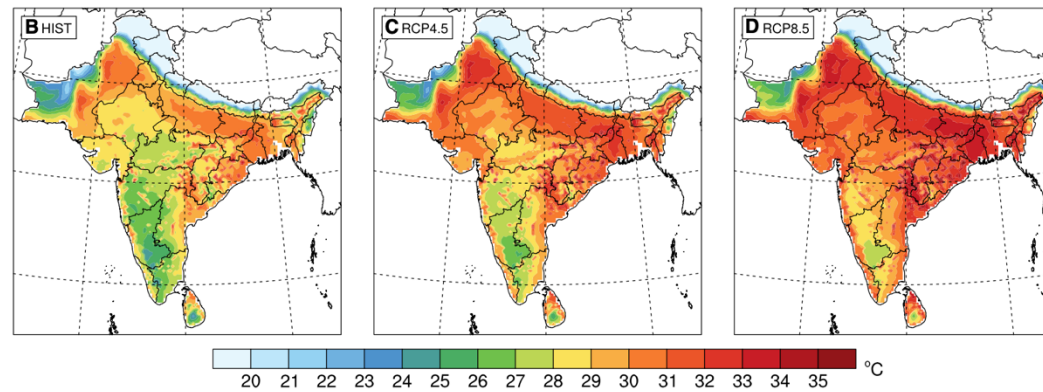


Figure 6. Twmax (°C), and maps of the ensemble averaged 30-year Twmax. The spatial distributions of bias-corrected ensemble averaged 30-year Twmax for each GHG scenario: HIST (1976–2005) (B), RCP4.5 (2071–2100) (C), and RCP8.5 (2071–2100) (D). This figure and legend are taken from Im et al. (2017) figure 2.

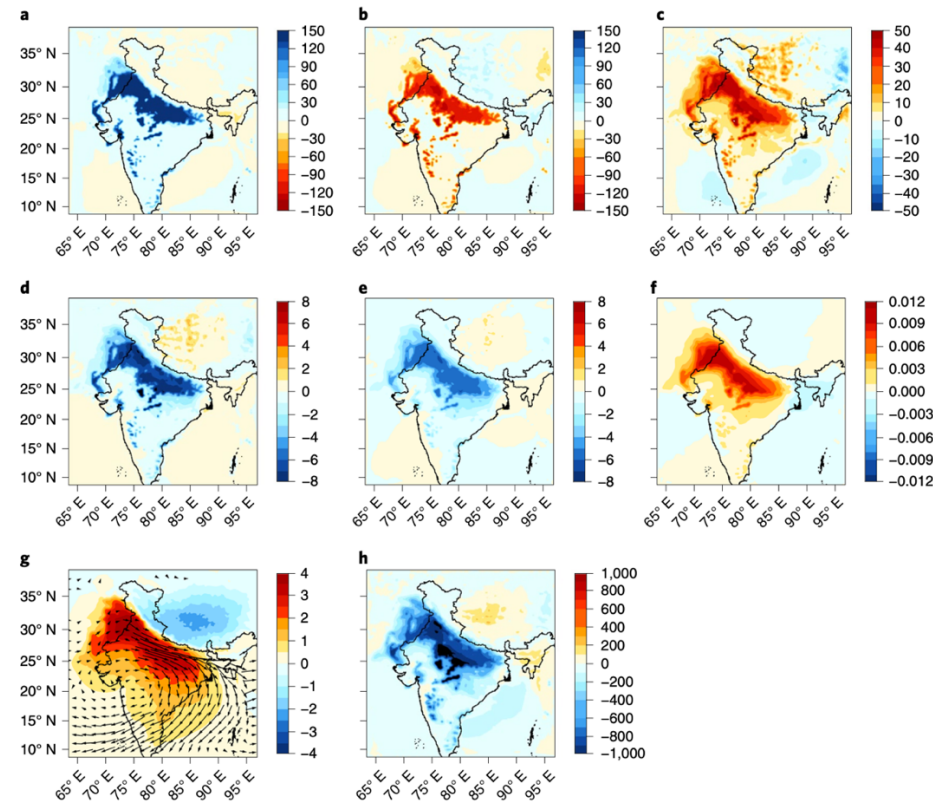


Figure 7. The role of irrigation on summer heat fluxes, temperature humidity SLP, and PBL height. All of the plots represent the irrigation minus no irrigation anomaly during 2000-2018. (a) latent heat (W m^{-2}), (b) sensible heat flux (W m^{-2}), (c) the sum of latent and sensible heat fluxes (W m^{-2}), (d) T_{LS} (K), (e) T_2 (K), (f) specific humidity (kg/kg), (g) SLP (hPa), (h) PBL height (m). This figure and legend are taken from Vimal et al. (2017) figure 3.

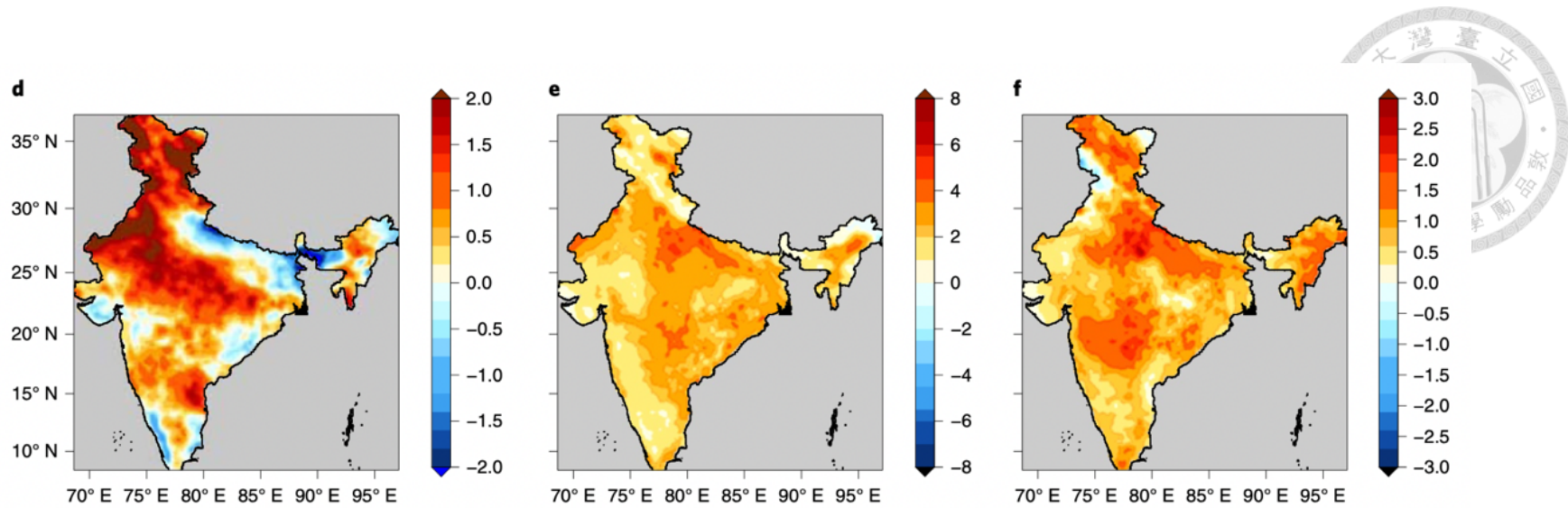


Figure 8. Changes in three days maximum heat indicators in India during April to May for 1979 to 2018 period. (d) Changes in the three days maximum T_2 ($^{\circ}\text{C}$), (e) Heat index ($^{\circ}\text{C}$), and (f) T_w ($^{\circ}\text{C}$). This figure and legend are taken from Vimal et al. (2017) figure 2.

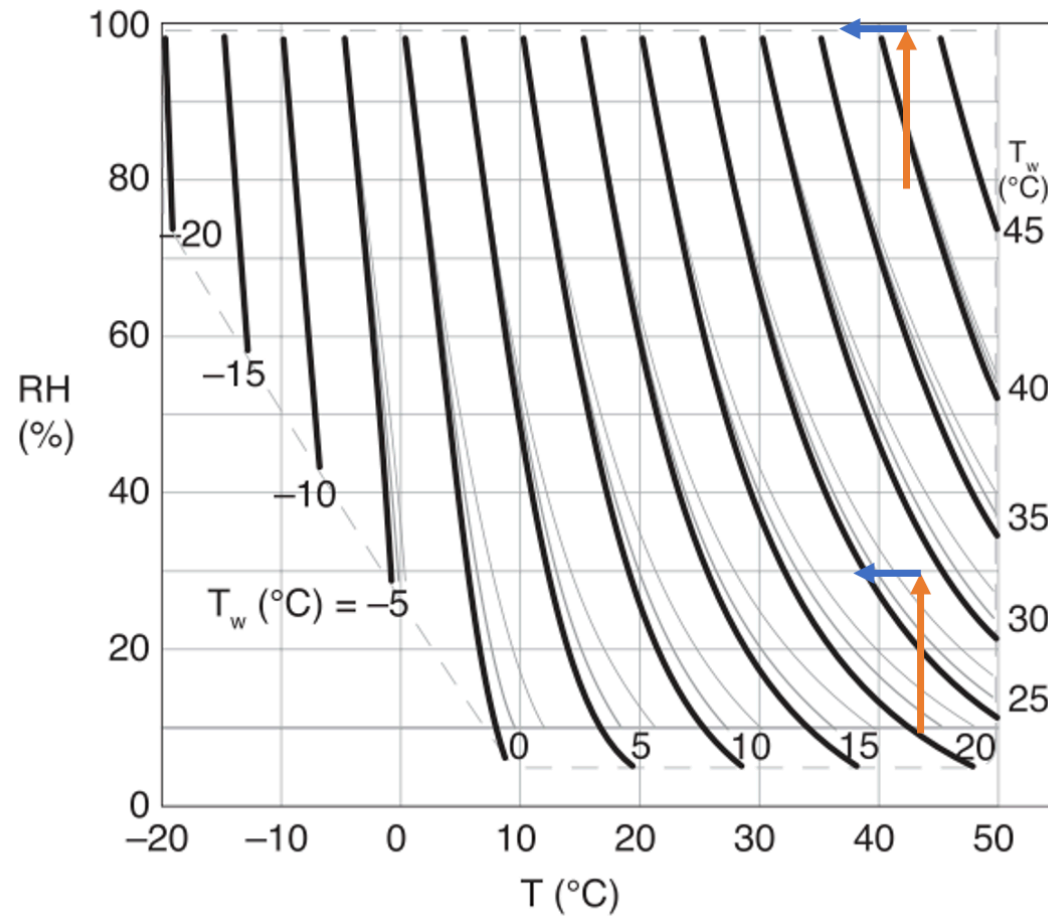


Figure 9. Isopleths of T_w versus RH% and T. This figure and legend are taken from Roland et al. (2011) figure 2. The orange arrow represents the moistening iteration and the blue arrow represents the cooling iteration. The arrows don't describe the real iteration of the change in T_w .

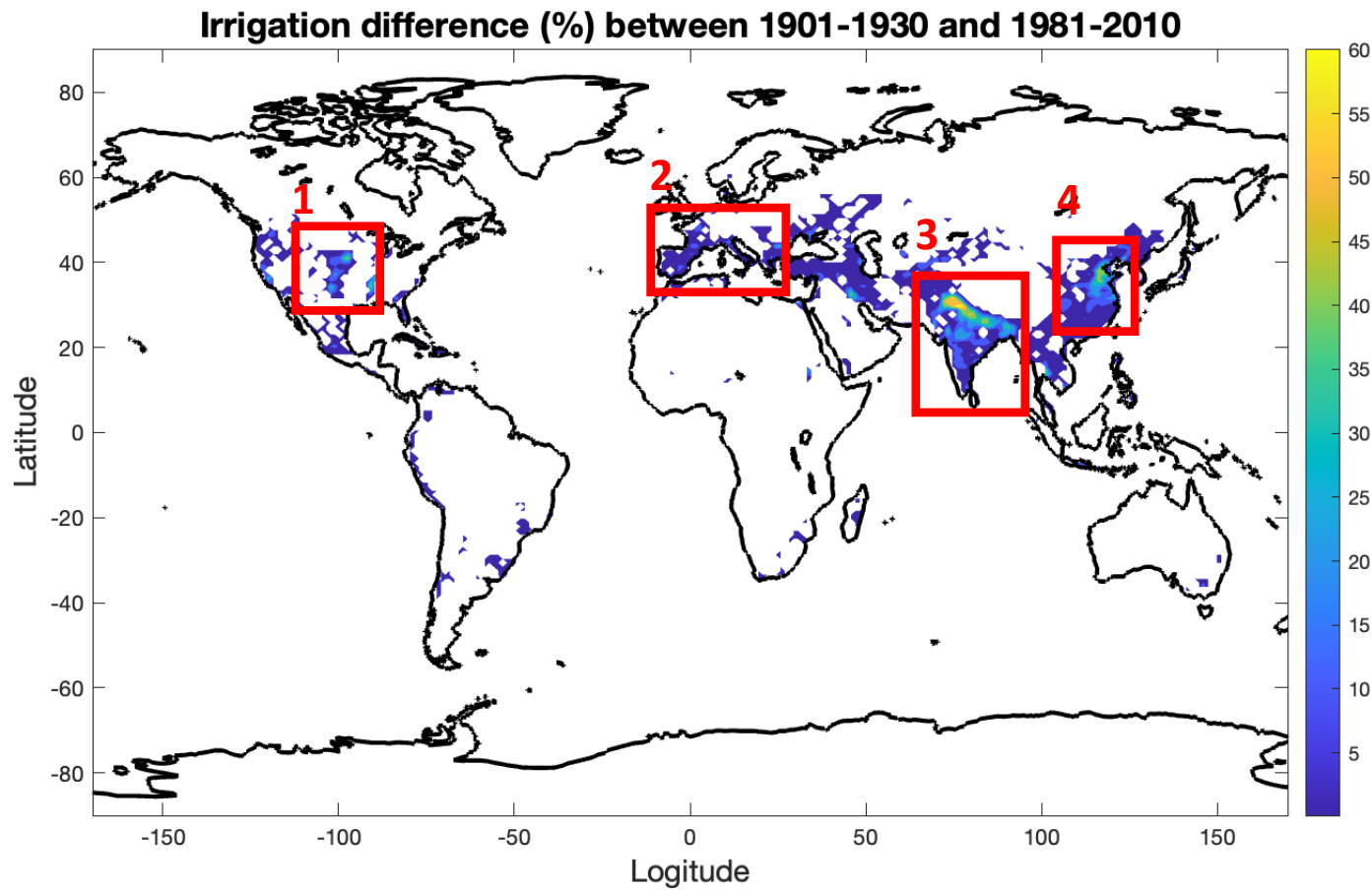


Figure 10. Irrigation fraction difference (%) between the early 20th century reference period (1901-1930) and present-day (1981-2010). The main irrigation change areas are situated in the red boxes, which are Central US, Europe, South Asia, and North China, respectively.

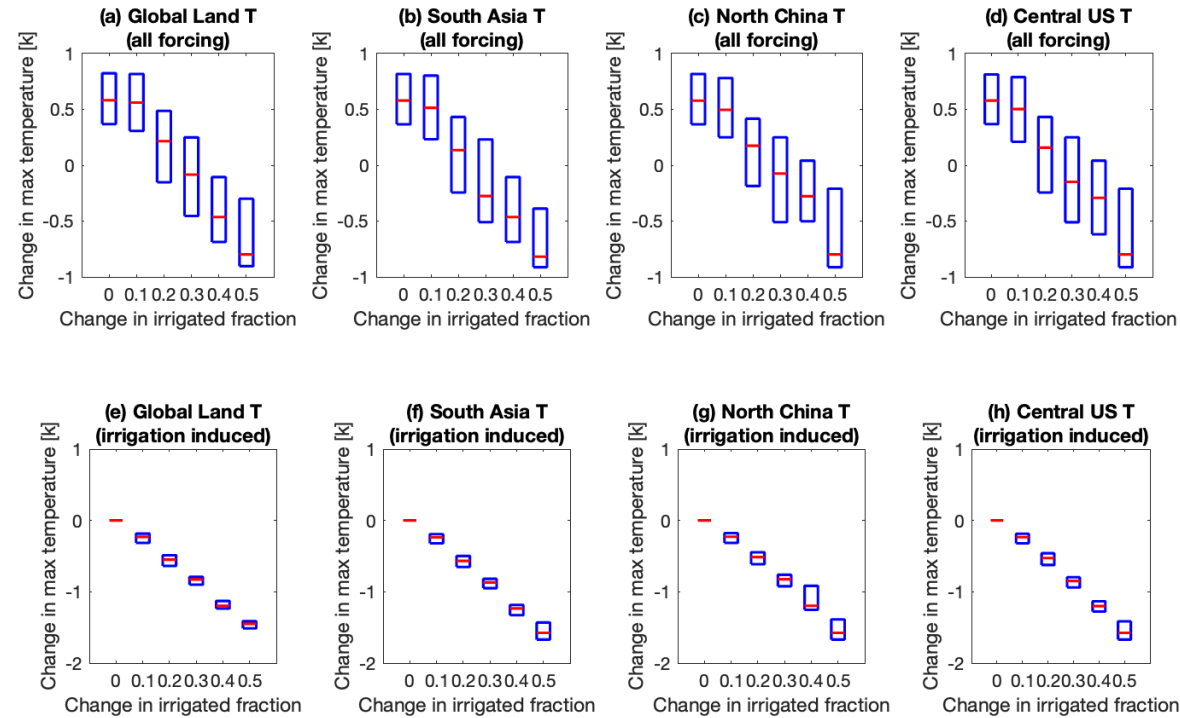


Figure 11. Change in ΔTX_m versus change in the irrigated fraction in Global land, South Asia, North China, and the Central USA. The delta symbol represents the difference between 1901-1930 and 1981-2010. (a) Global land (all), (b) South Asia (all), (c) North China (all), (d) Central US (all), (e) Global land (irrigation induced only), (f) South Asia (irrigation induced only), (g) North China (irrigation induced only), (h) Central US (irrigation induced only).



Global Land Profile

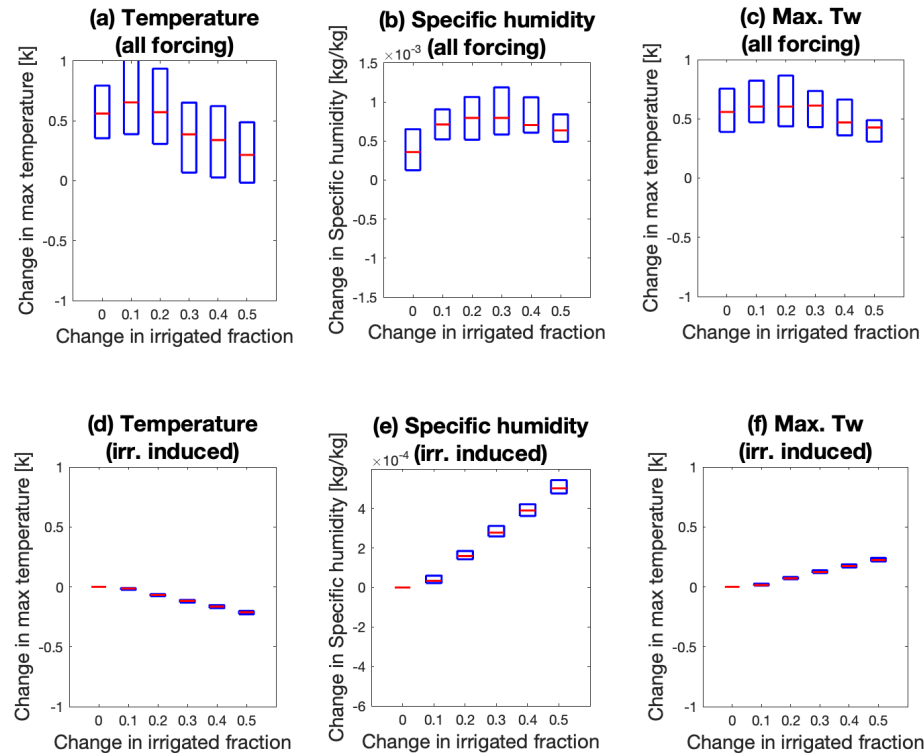


Figure 12. Change in temperature (K), specific humidity (kg/kg), and maximum wet-bulb temperature (K) in Global land. Note that the time of temperature and specific humidity are selected the same as the maximum wet-bulb temperature. (a) temperature (all), (b) specific humidity (all), (c) wet-bulb temperature (all), (d) temperature (irrigation induced only), (e) specific humidity (irrigation induced only), (f) wet-bulb temperature (irrigation induced only).



Central US Profile

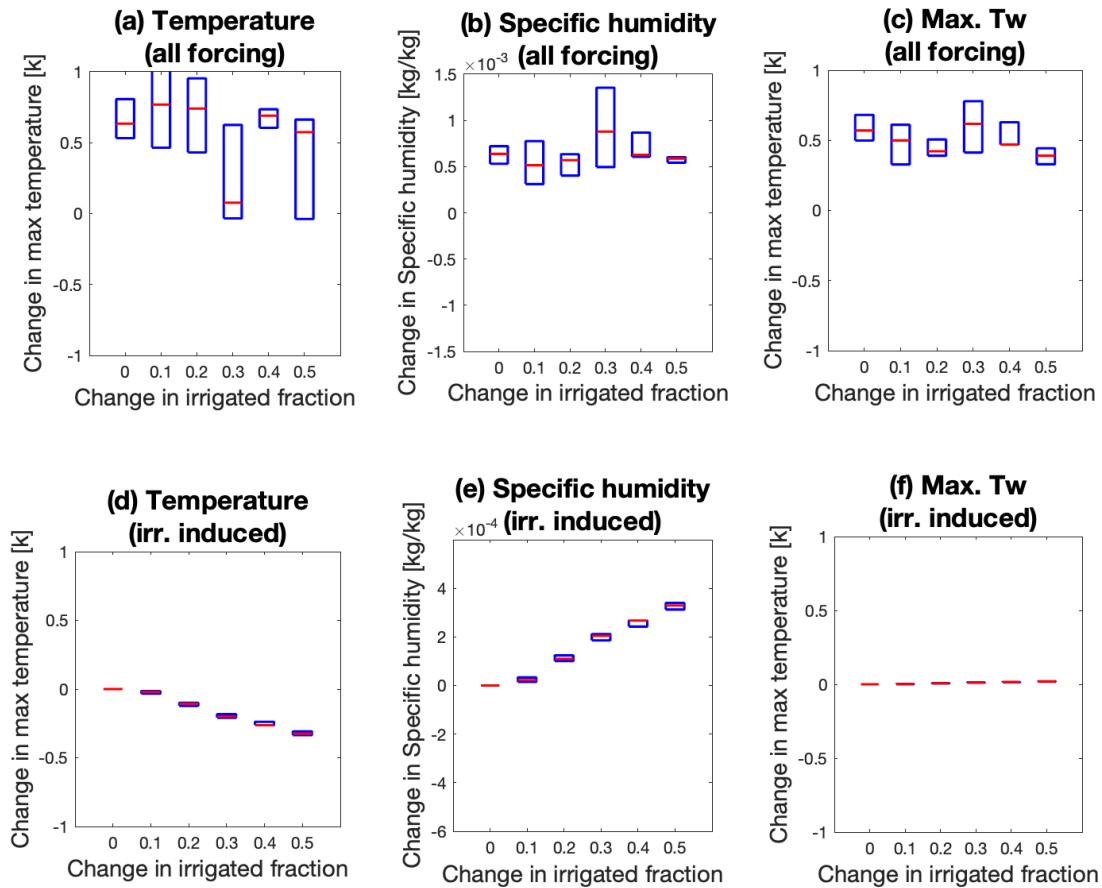


Figure 13. Same as figure 12, but for Central US.

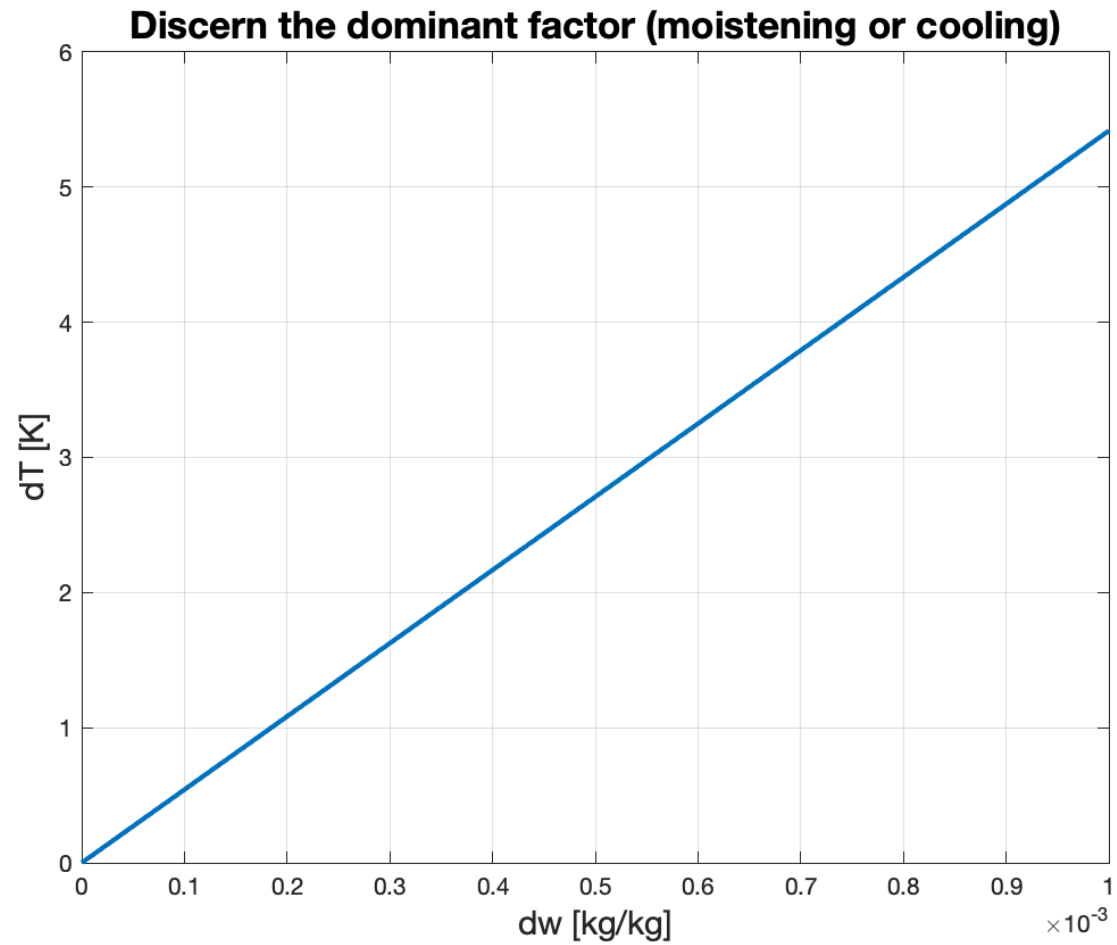


Figure 14. The equivalent effect of increasing mixing ratio on dry-bulb temperature change.



North China Profile

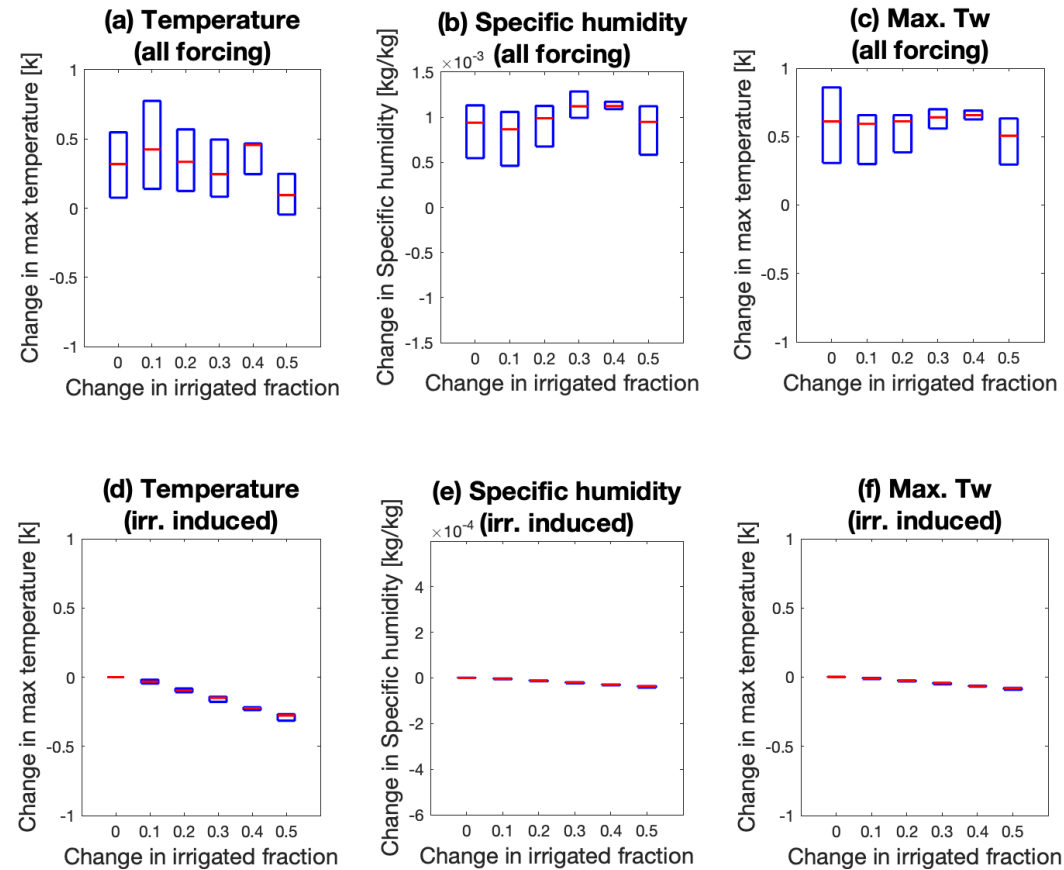


Figure 15. Same as figure 12, but for North China.



Europe Profile

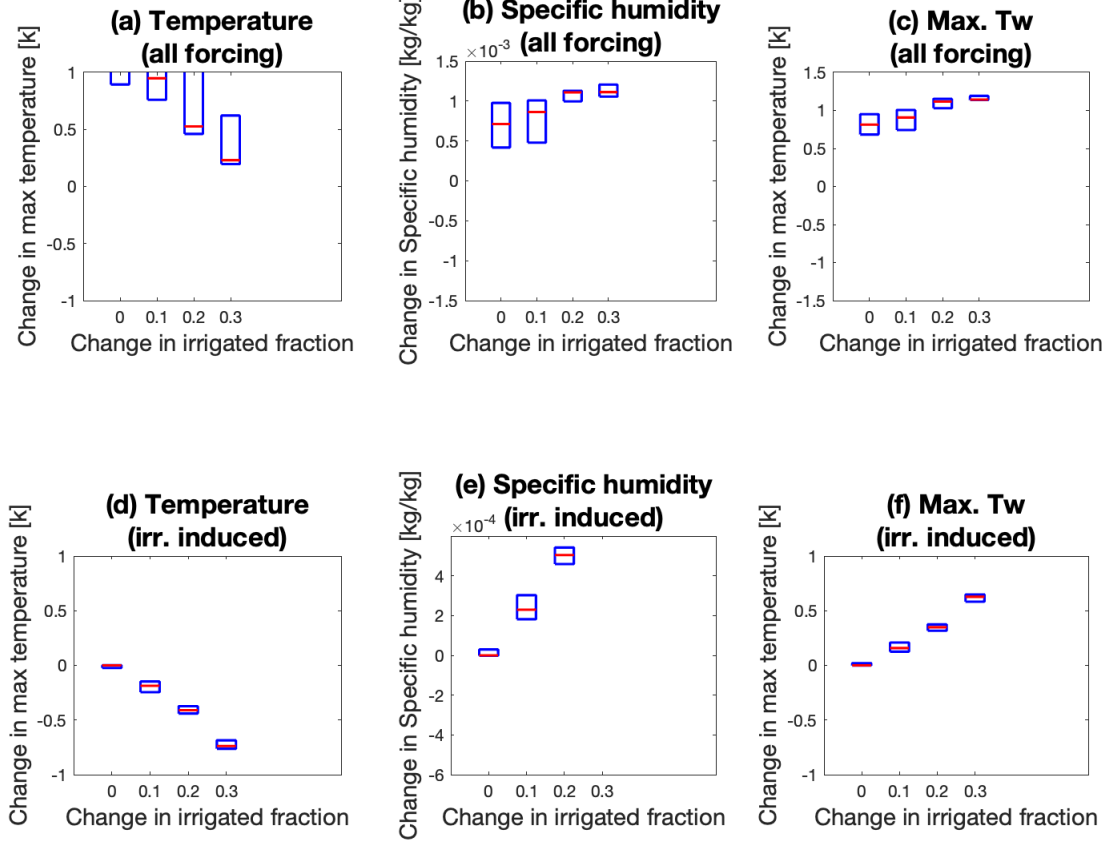


Figure 16. Same as figure 12, but for Europe.



South Asia Profile (Wet Season)

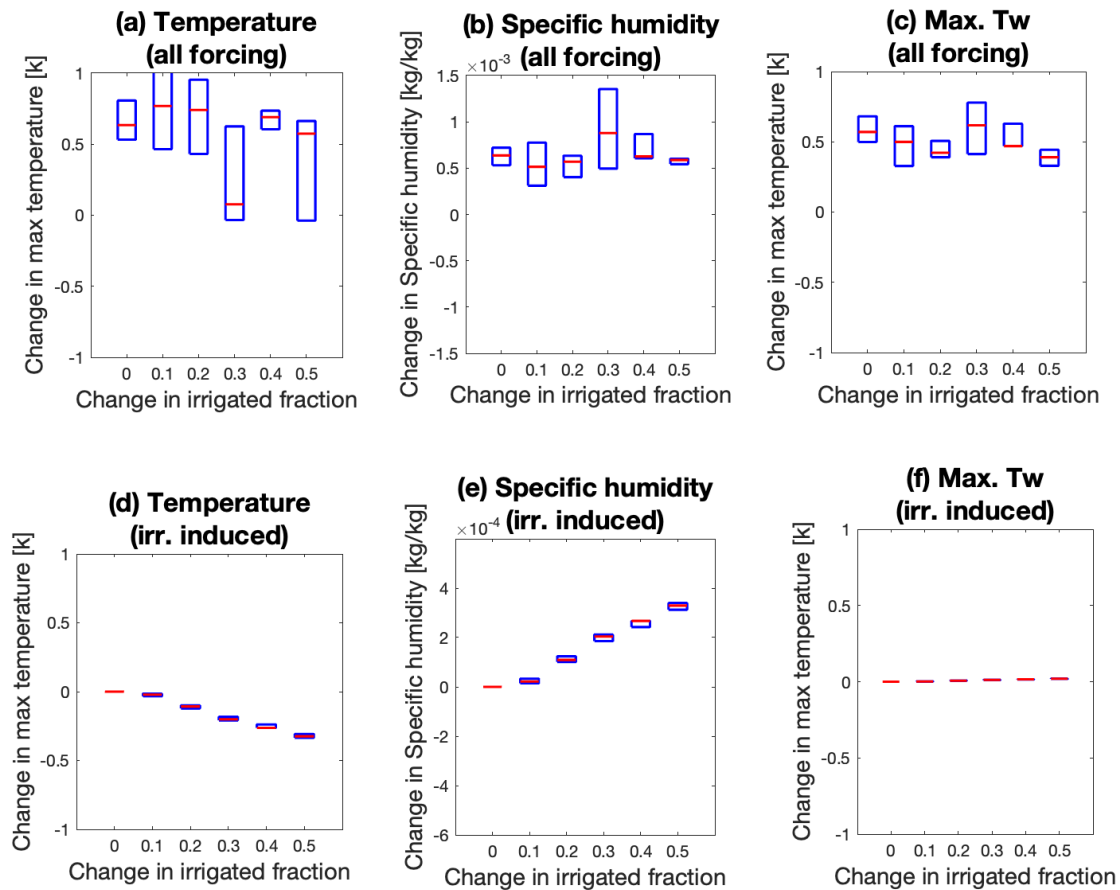


Figure 17. Same as figure 12, but for wet seasons in South Asia.

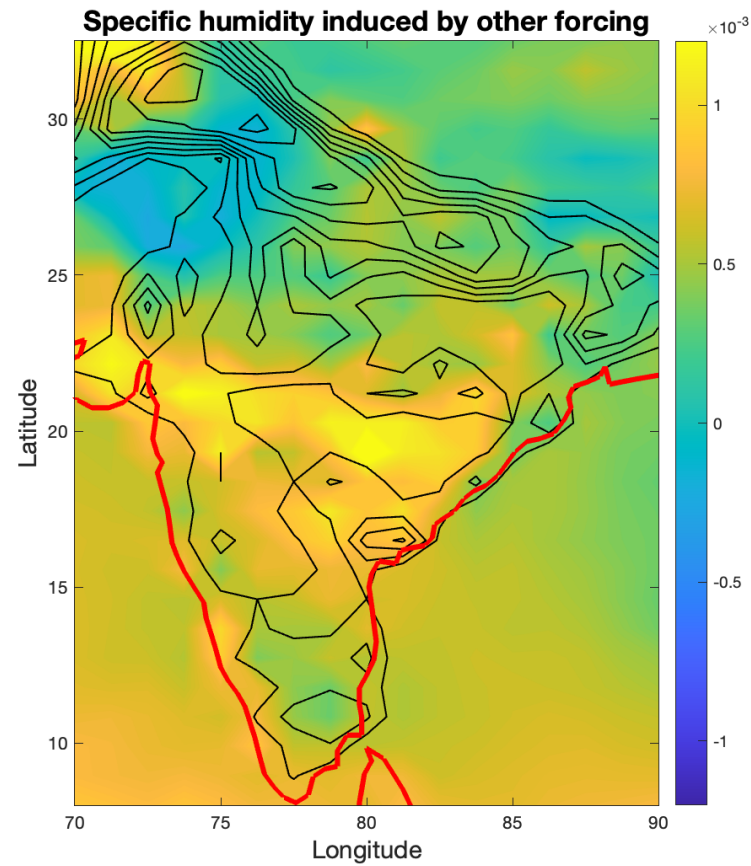


Figure 18. The specific humidity (kg/kg) changes due to other forcing. The contour represents the irrigation fraction from 1981 to 2010 and the red line is the coastline of India. Note that most of the irrigation area is located in Northwest India.



South Asia Profile (Dry Season)

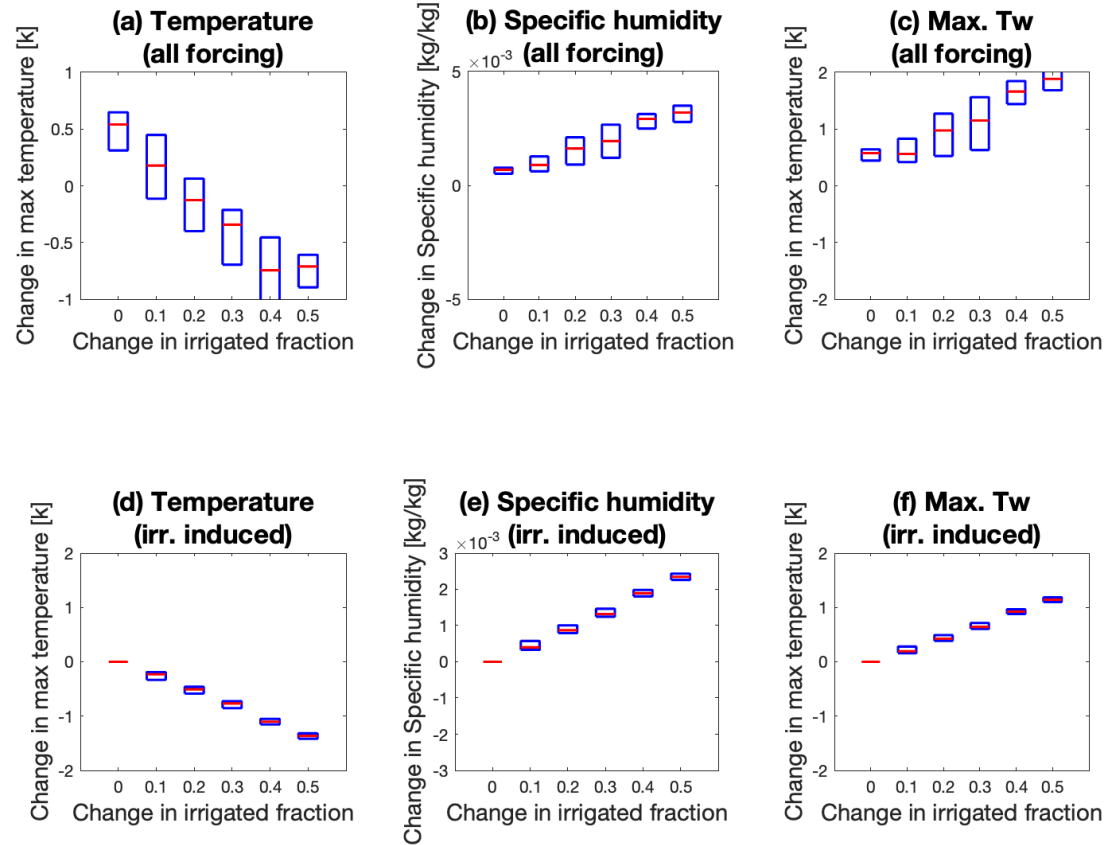


Figure 19. Same as figure 12, but for dry seasons in South Asia.

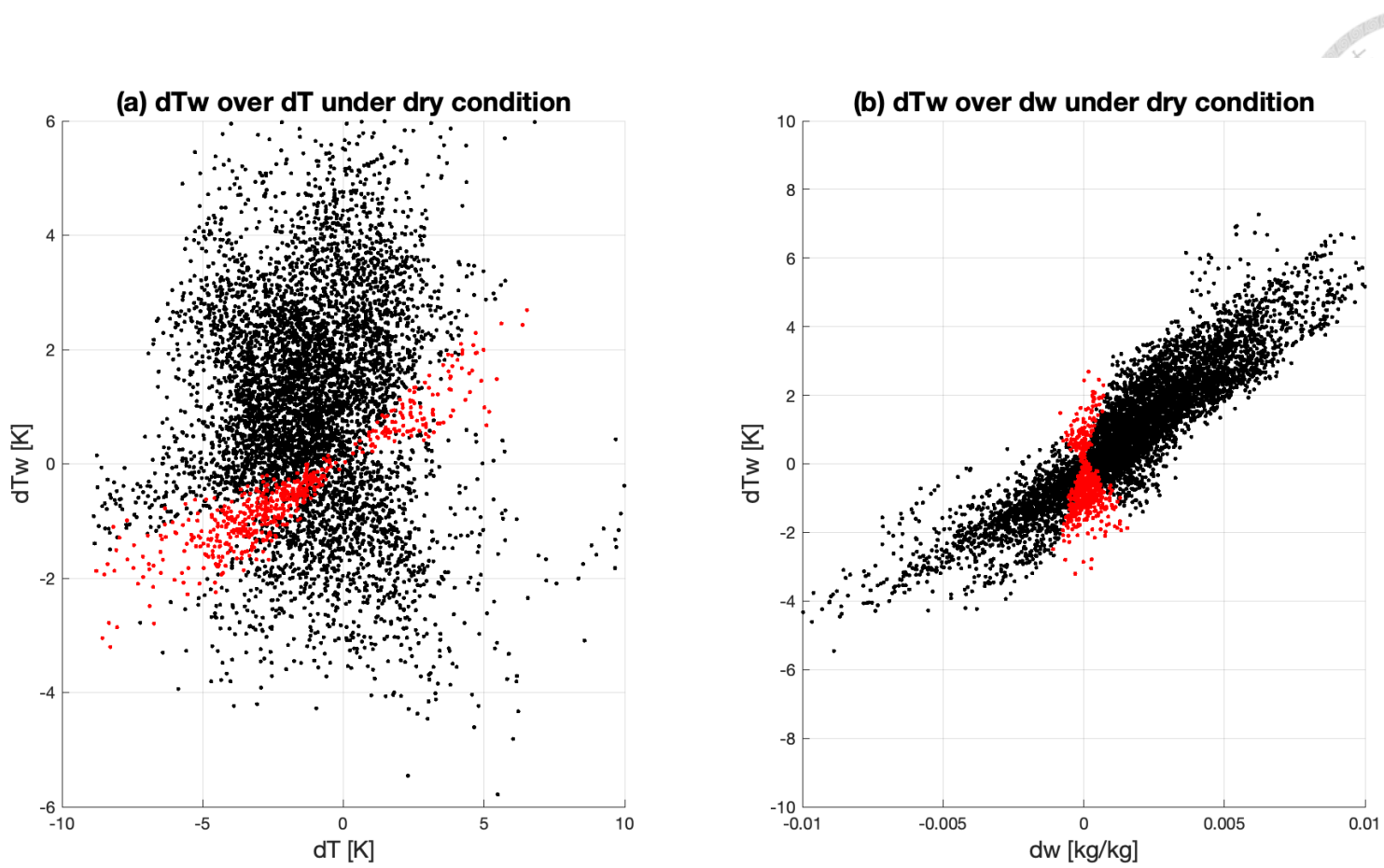


Figure 20. Irrigation effect of one month average in dry South Asia (1981-2010). The criteria are RH lower than one standard deviation. (a) Tw change over temperature change. (b) Tw change over mixing ratio change. Note that red dots represent the temperature effect is larger than the mixing ratio.

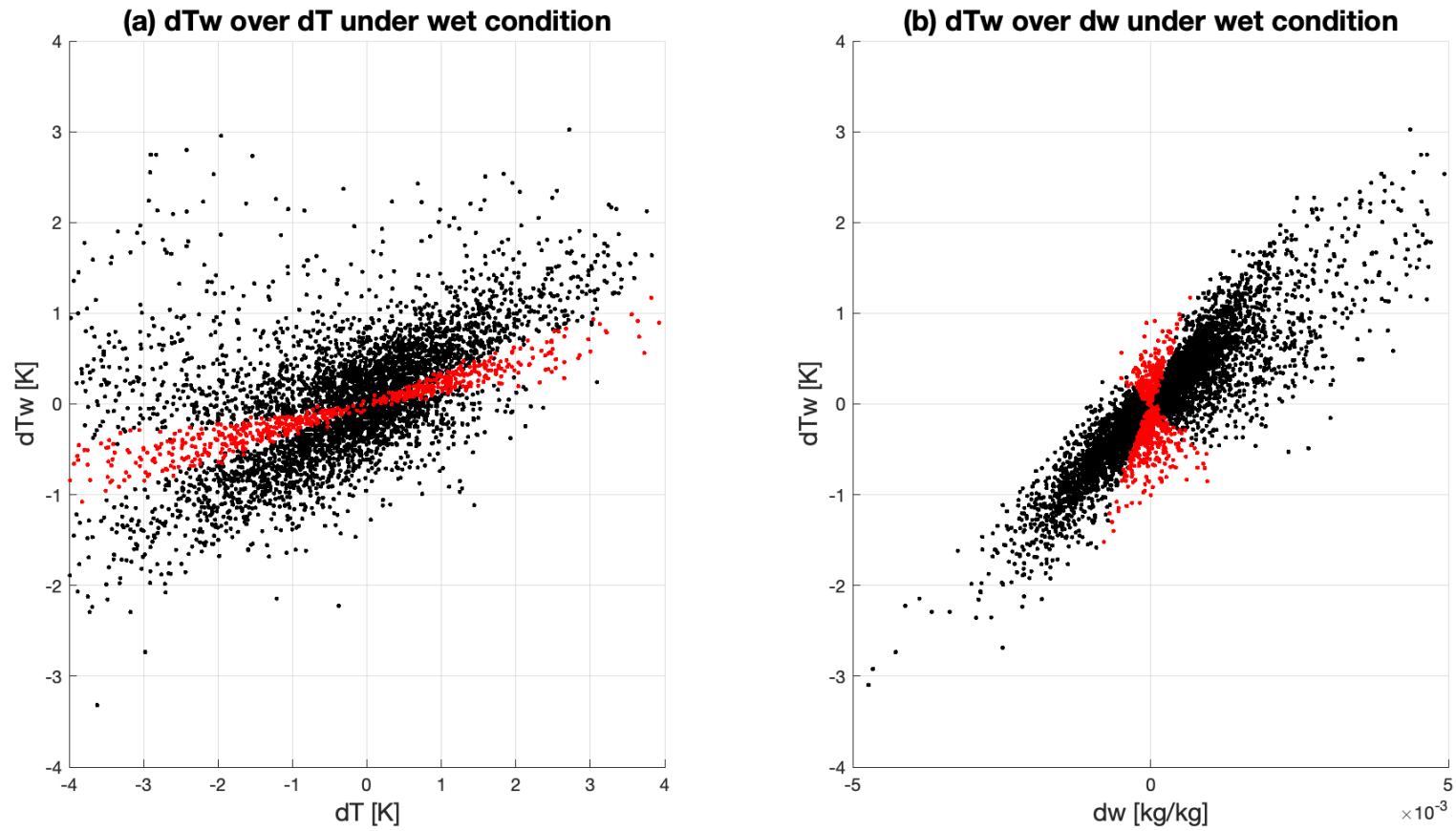


Figure 21. Same as figure 20, but the criteria are RH higher than one standard deviation which represents as wet South India.

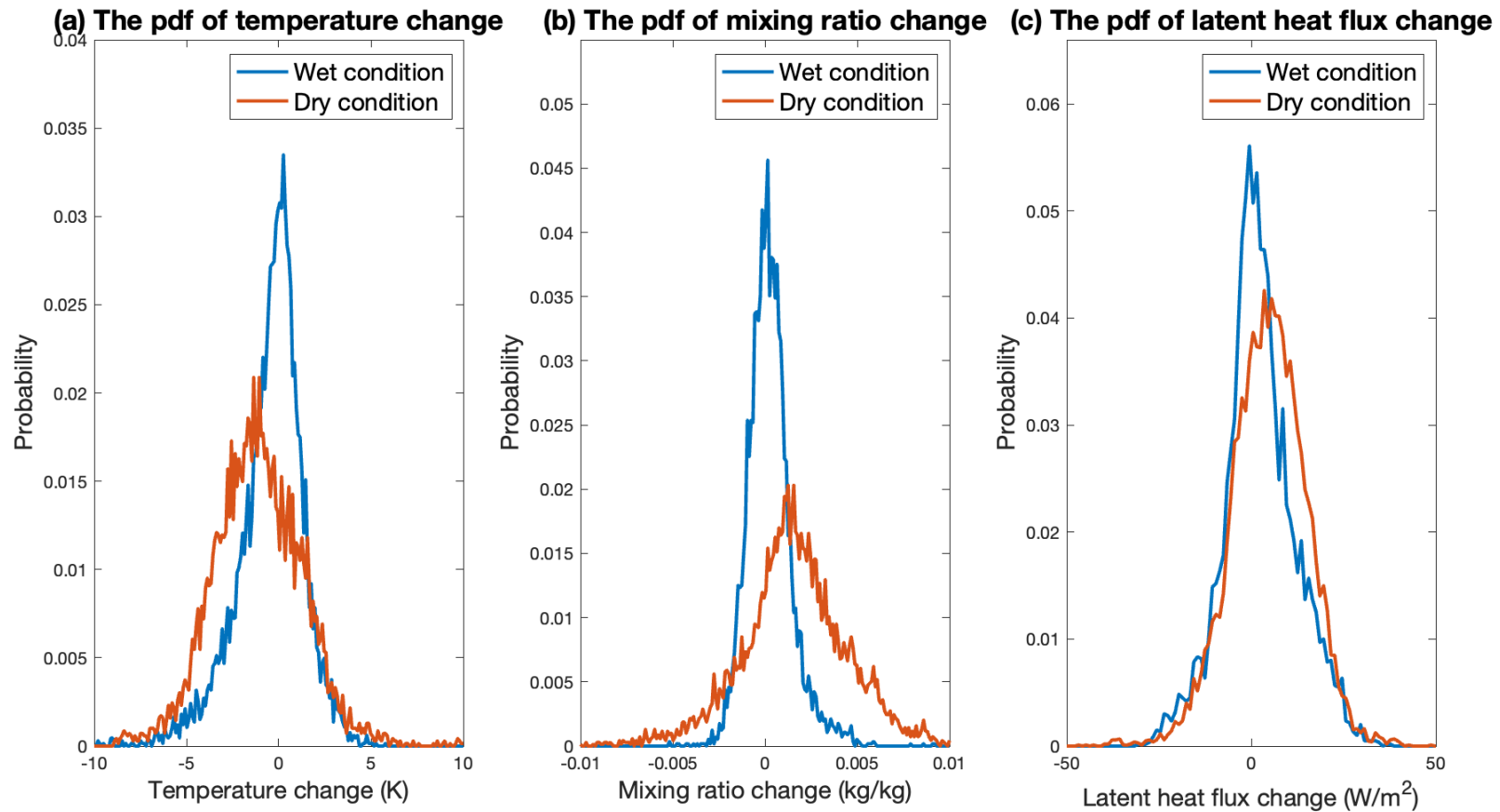


Figure 22. The probability density function of (a) temperature change (K), (b) mixing ratio (kg/kg), (c) latent heat flux (W/m²) in wet and dry conditions. The criteria for dry and wet conditions are the same as figures 20 and 21.

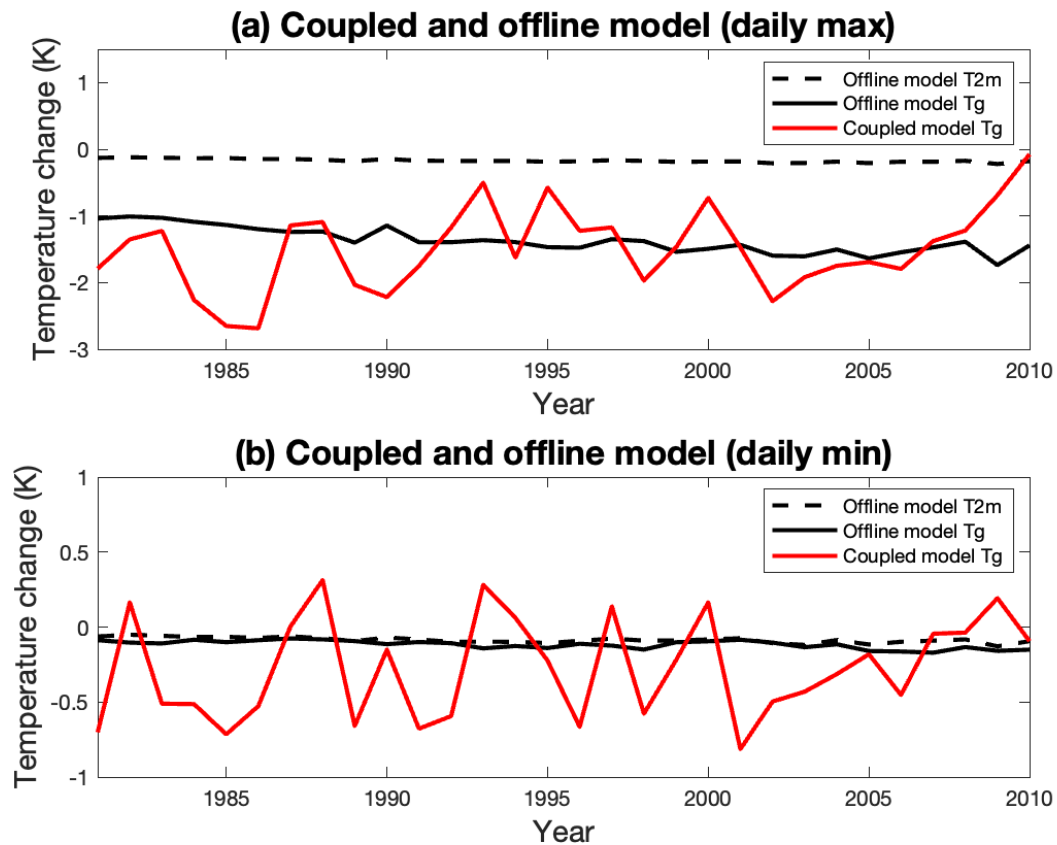


Figure 23. Comparison between the coupled and offline models in daily maximum and minimum in South Asia. The temperature change is irrigation run minus control run (1981 to 2010). (a) The annual mean of the daily maximum temperature between 1981 to 2010. (b) The annual mean of the daily minimum temperature between 1981 to 2010.

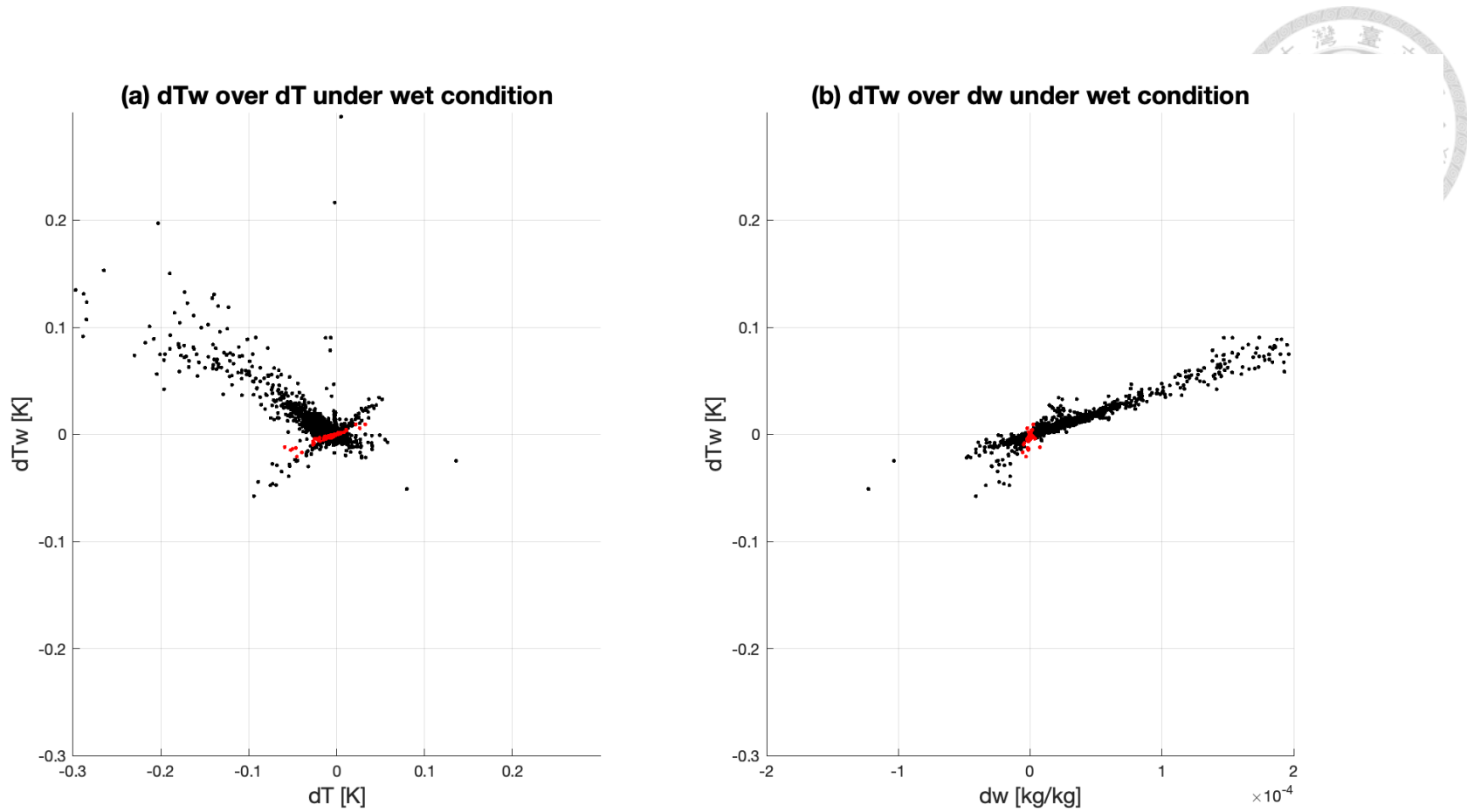


Figure 24. Irrigation effect of one month average in wet South Asia of the offline model (1906-2014). The criteria are RH higher than one standard deviation. (a) Tw change over temperature change. (b) Tw change over mixing ratio change. Note that red dots represent the temperature effect is larger than the mixing ratio.

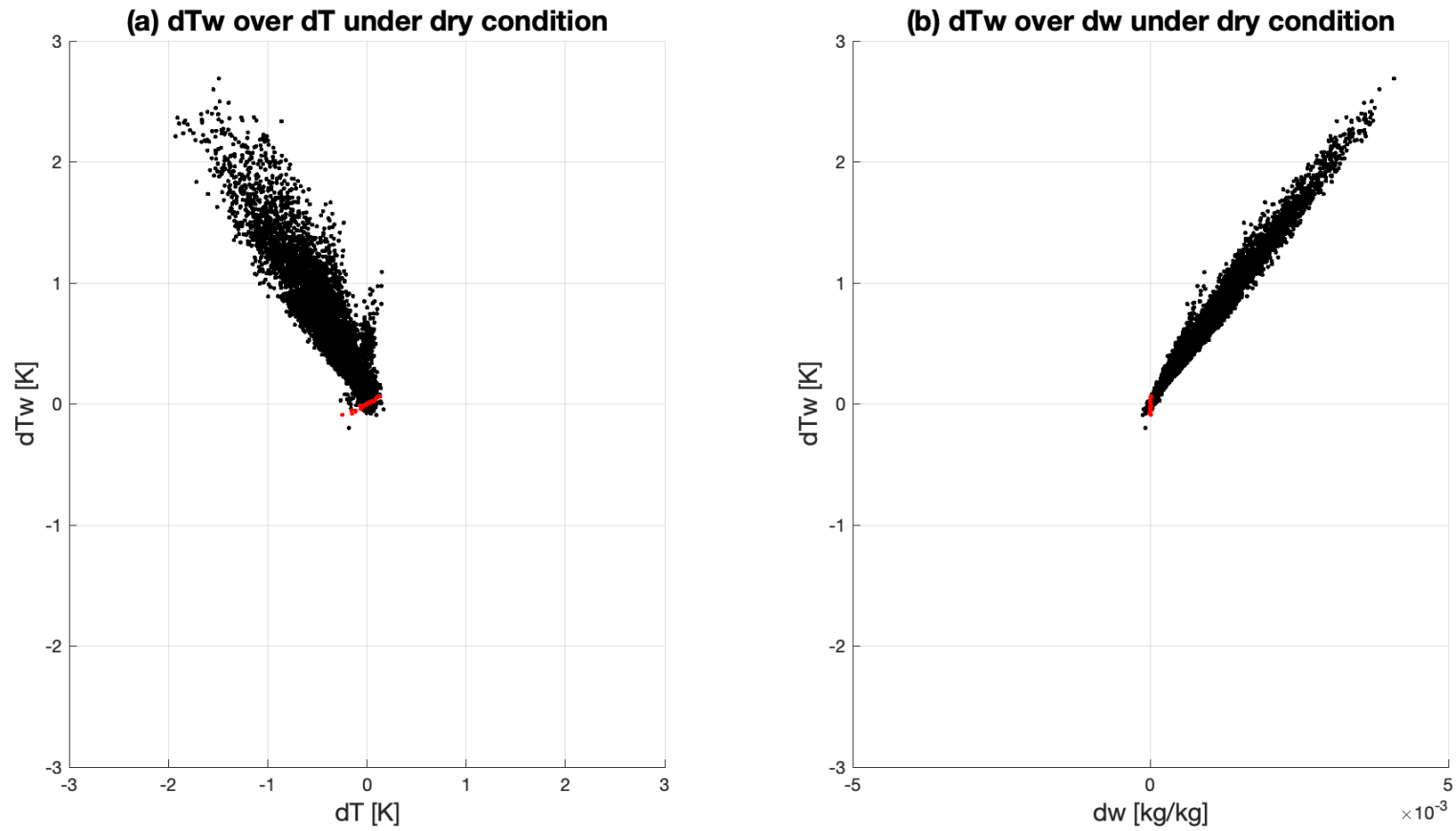


Figure 25. Same as figure 24, but the criteria are RH lower than one standard deviation which represents dry South India.

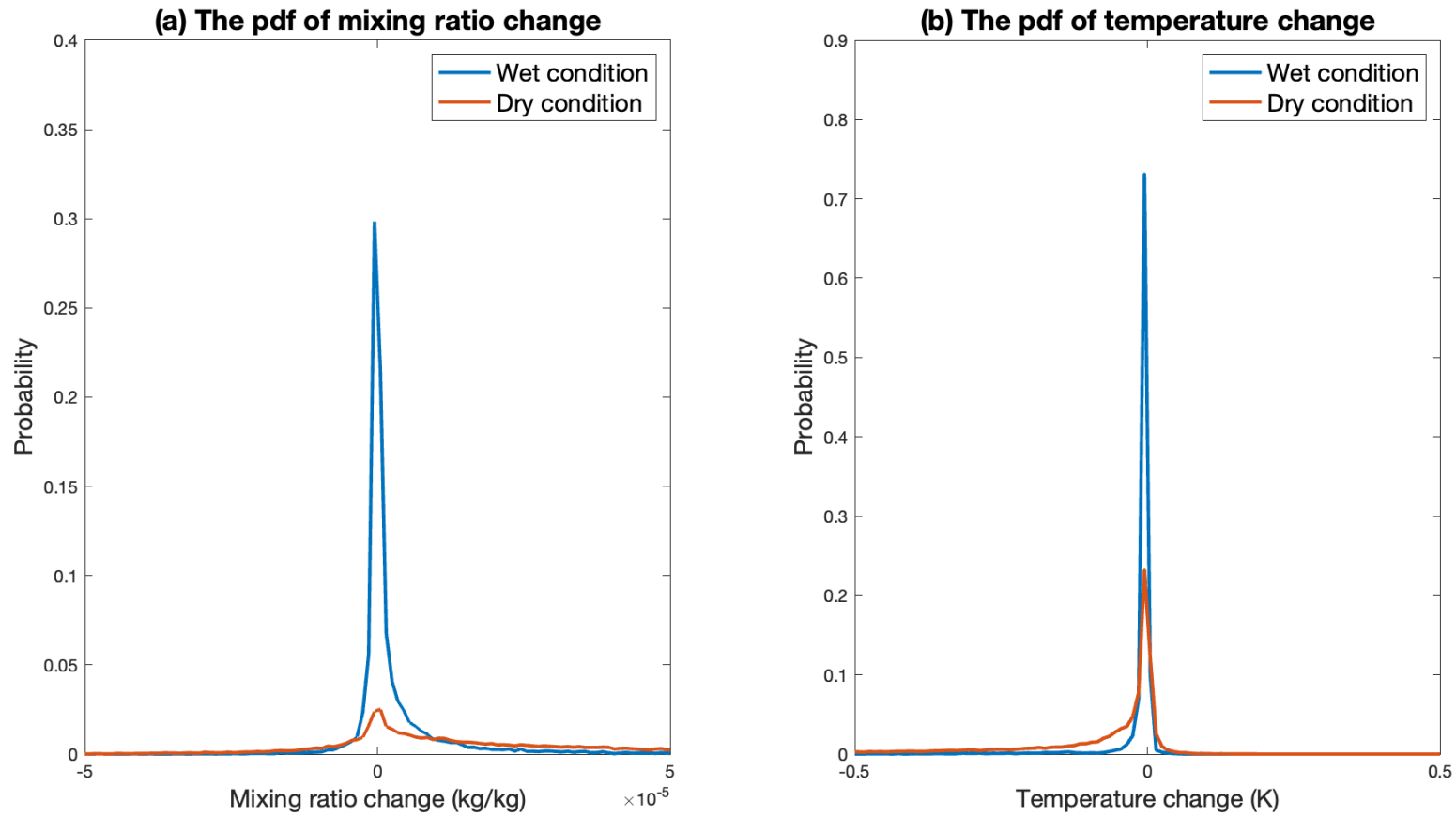
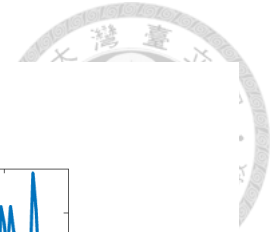


Figure 26. The probability density function of (a) mixing ratio change, (b) temperature in wet (blue line) and dry seasons (red line).



South Asia dry season profile

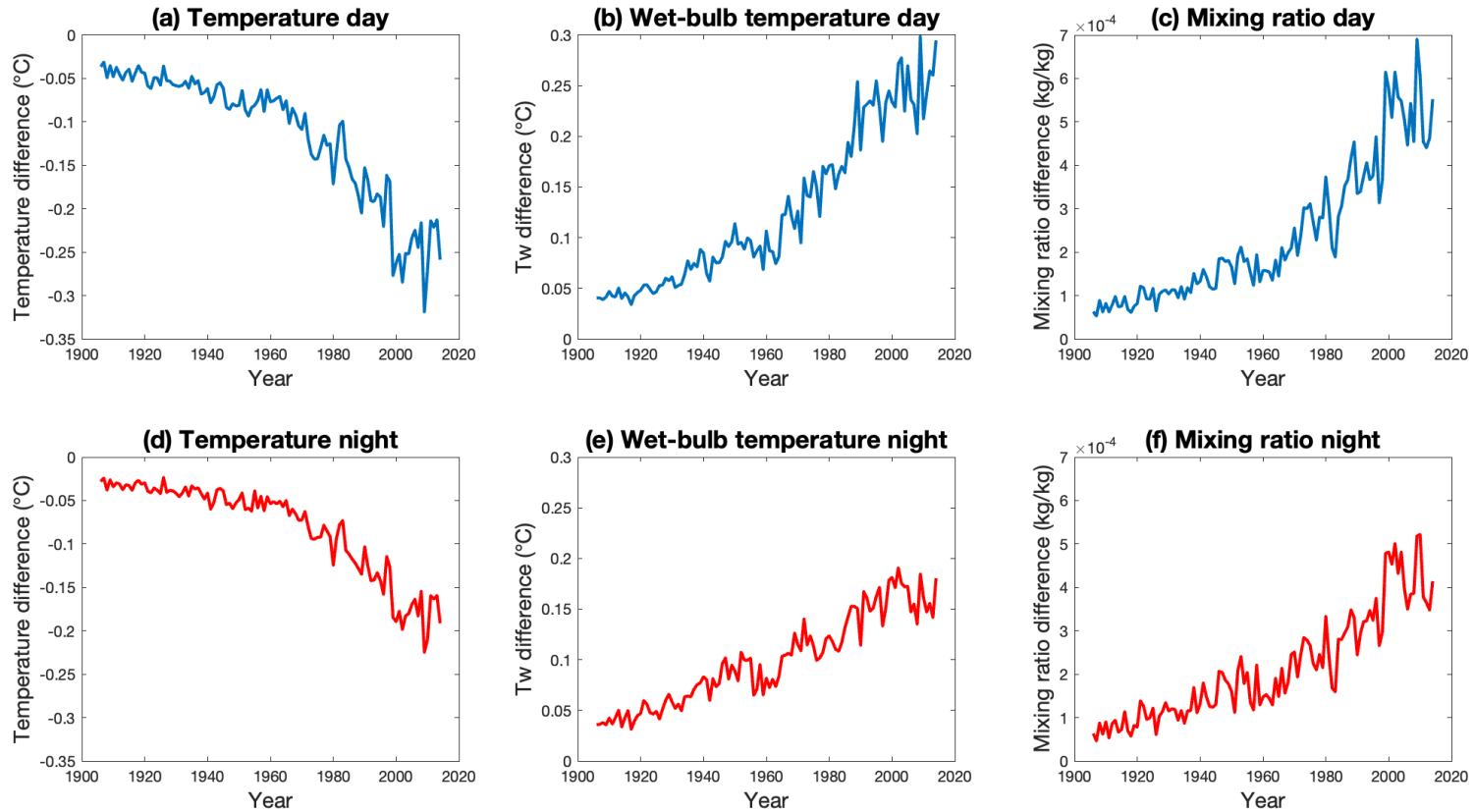


Figure 27. Each variable difference due to irrigation from 1906 to 2010 in the dry season of South Asia. Note that the blue lines represent daytime and red lines represent nighttime. (a) and (d) temperature, (b) and (e) wet-bulb temperature, (c) and (f) mixing ratio.



South Asia wet season profile

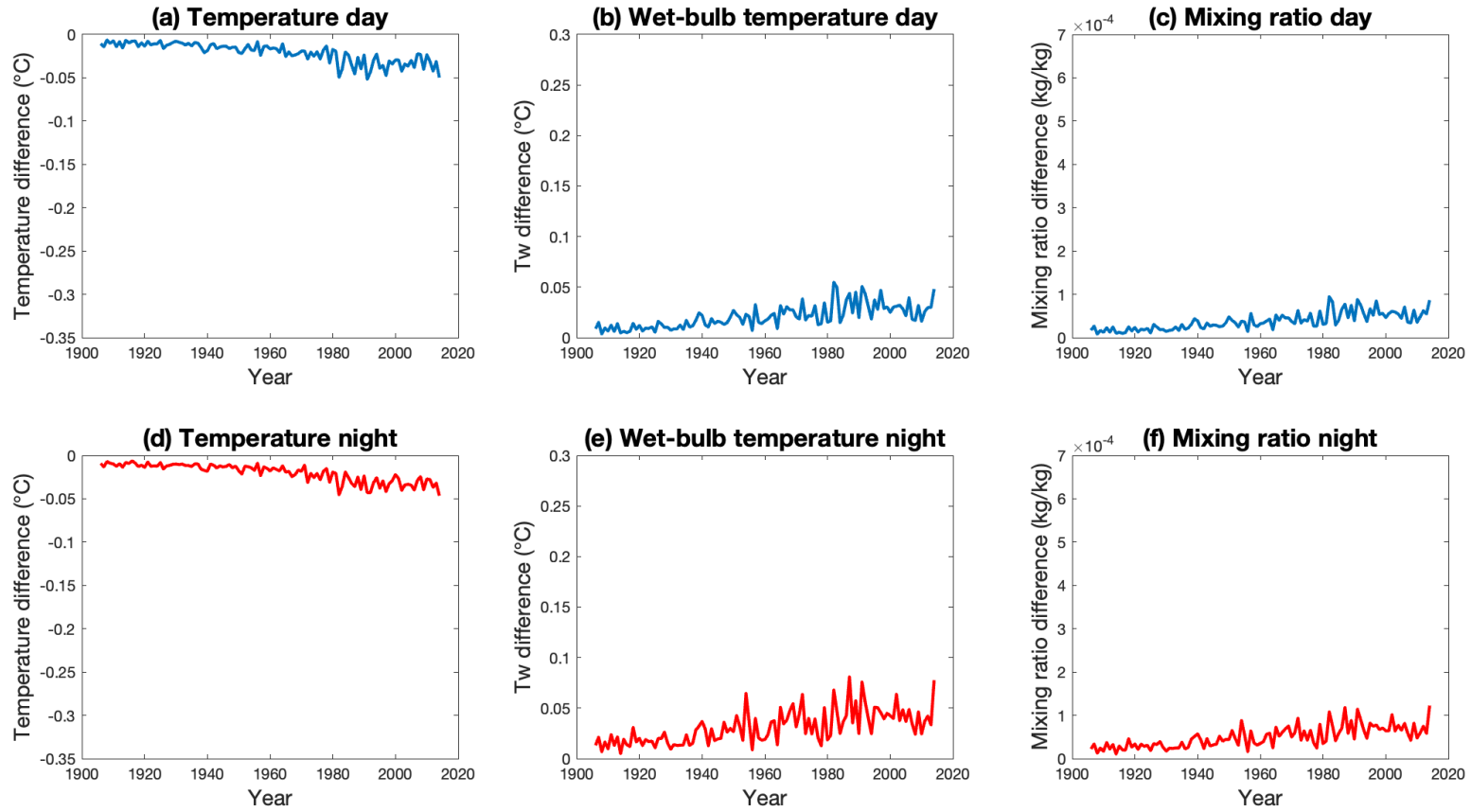


Figure 28. The same as figure 27, but for the wet season in South Asia.

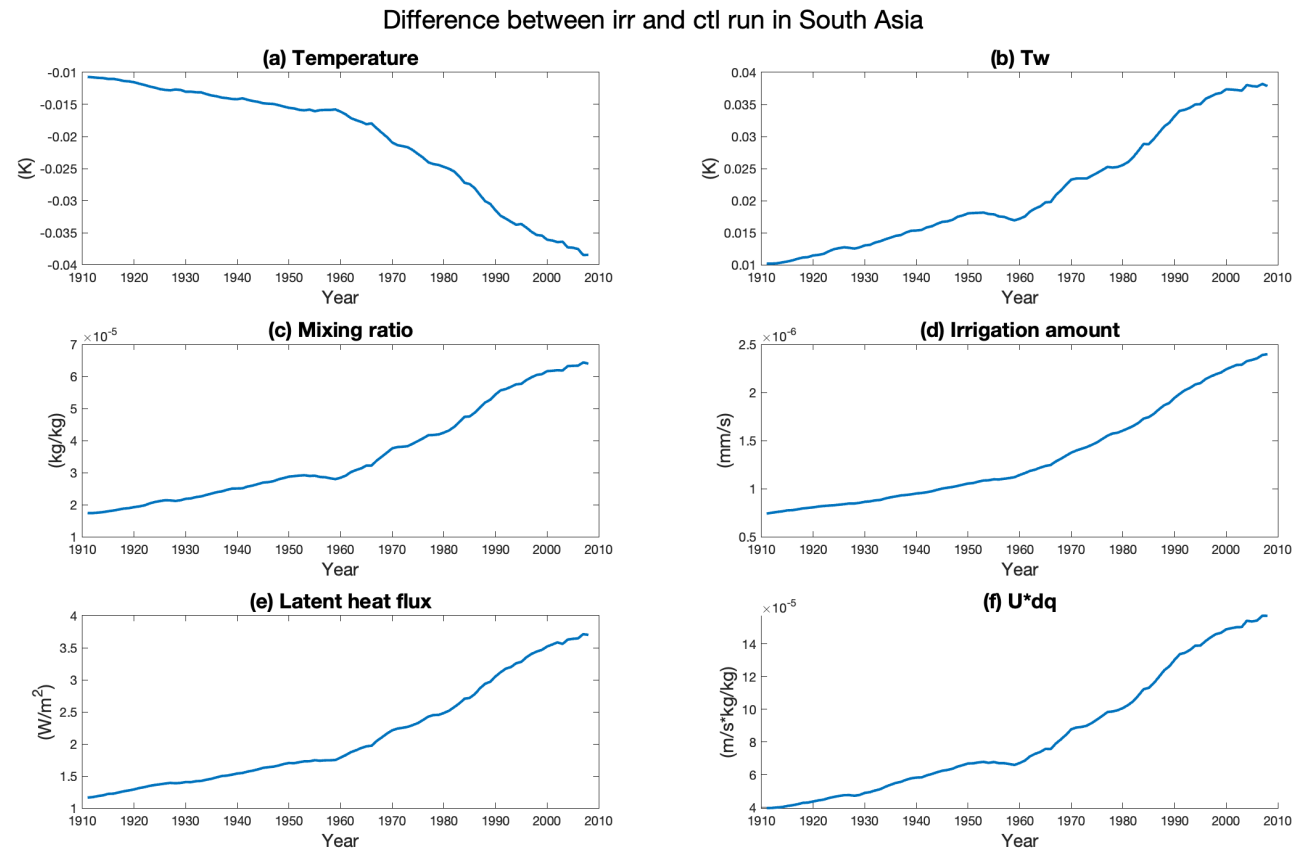


Figure 29. Variables difference affected by irrigation in South Asia. (a) Temperature (K), (b) wet-bulb temperature (K), (c) mixing ratio (kg/kg), (d) irrigation amount (mm/s), (e) latent heat flux (W/m²), (f) mean wind speed in 10 m high times specific humidity difference.



Difference between irr and ctl run in North China

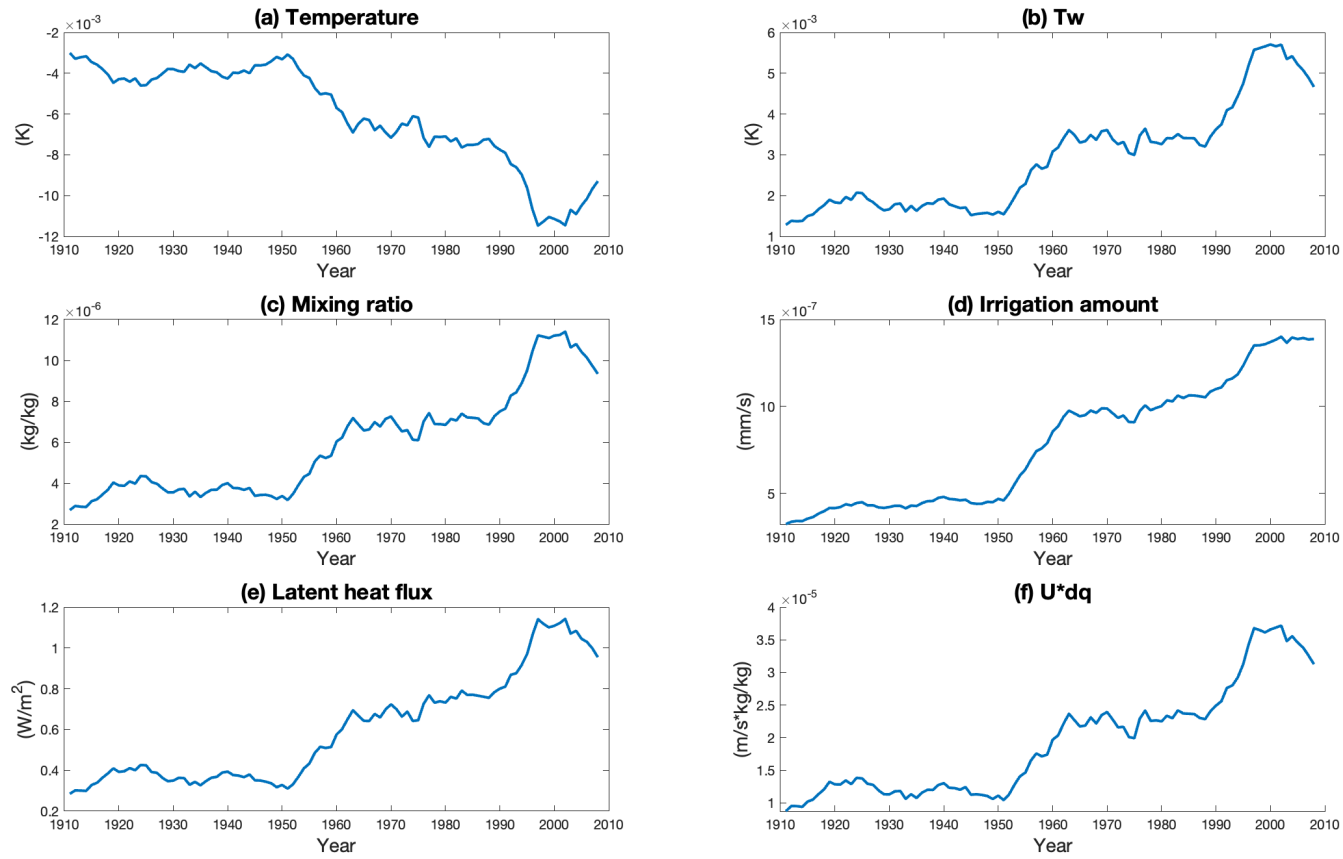


Figure 30. The same as figure 29, but for North China.

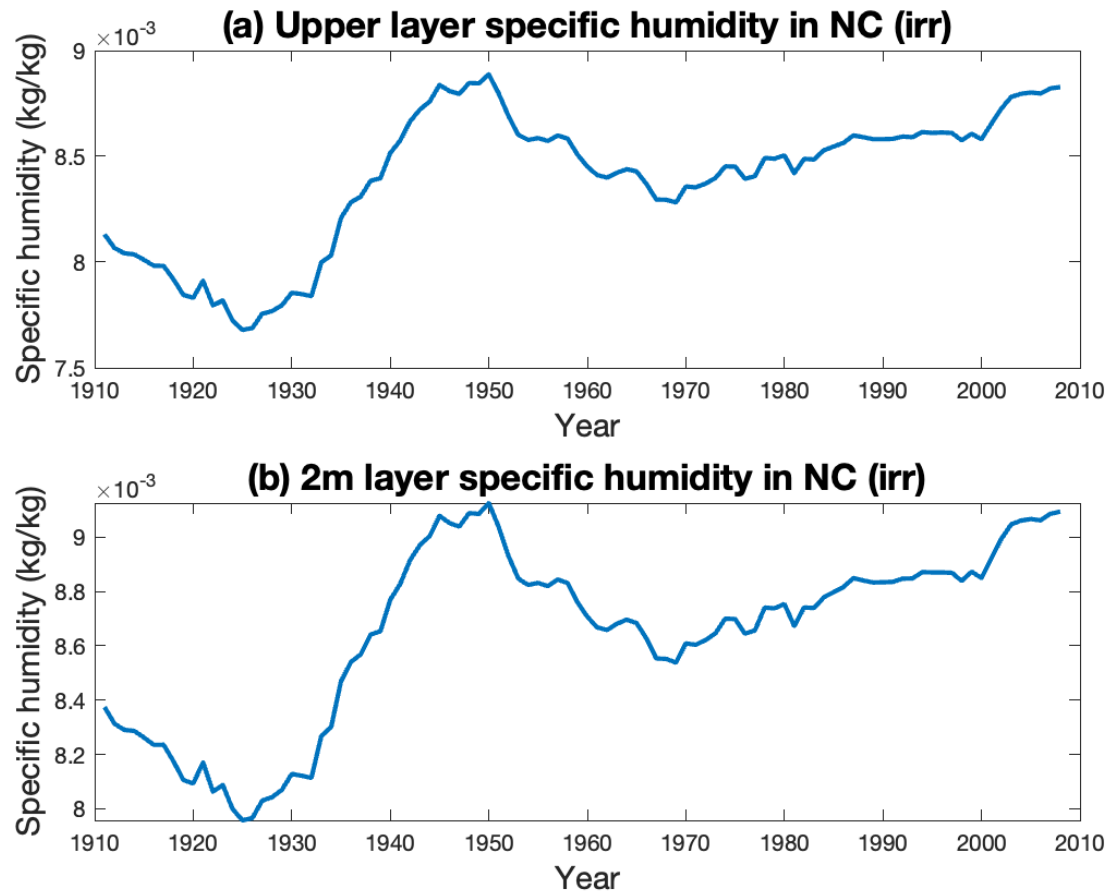


Figure 31. The specific humidity of different layers in North China over time. (a) Upper layer specific humidity in irrigation run (kg/kg), (b) 2m layer specific humidity in irrigation run (kg/kg).

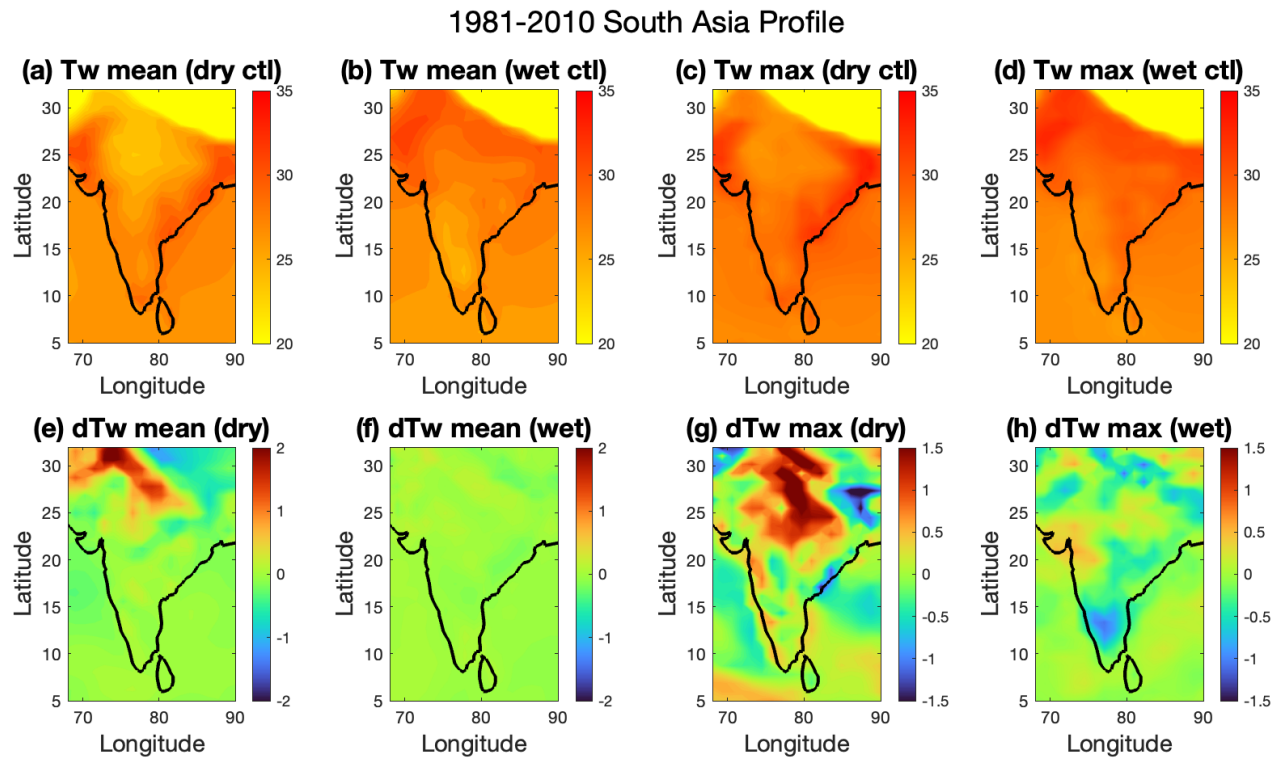


Figure 32. South Asia profile in 1981-2010 for dry and wet seasons in control run and the difference between irrigation and control analysis. (a) Tw mean for dry season and control run, (b) Tw mean for wet season and control run, (c) Tw maximum for dry season and control run, (d) Tw maximum for wet season and control run, (e) Tw difference between irr and ctl run in dry season, (e) Tw difference between irr and ctl run in dry season, (e) Tw difference between irr and ctl run in wet season, (g) Tw maximum difference between irr and ctl run in dry season, (h) Tw maximum difference between irr and ctl run in wet season.

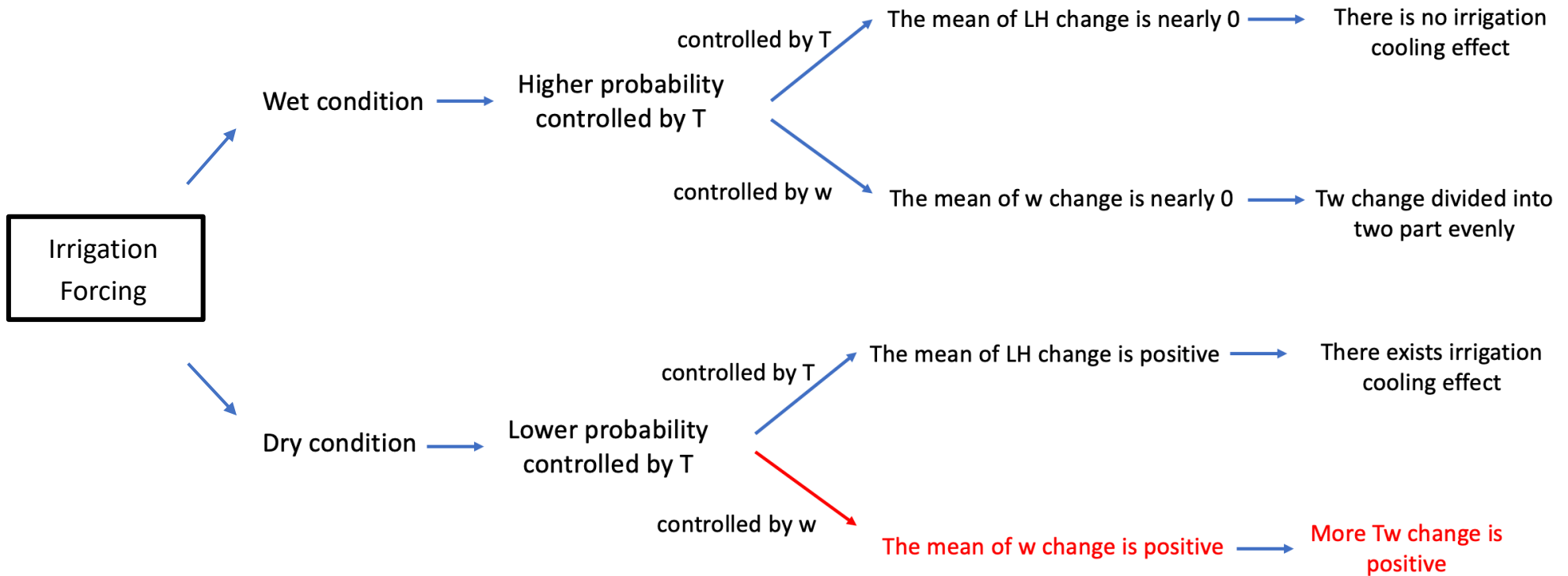
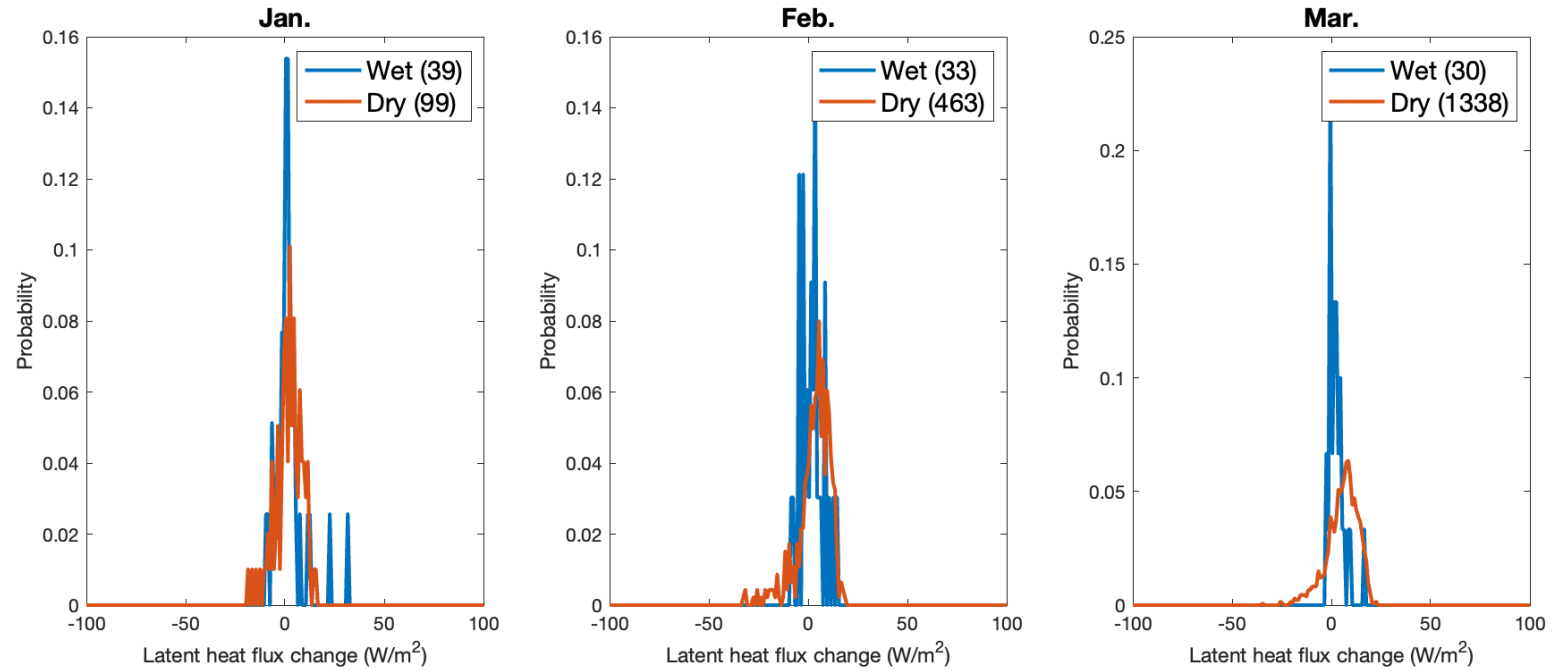
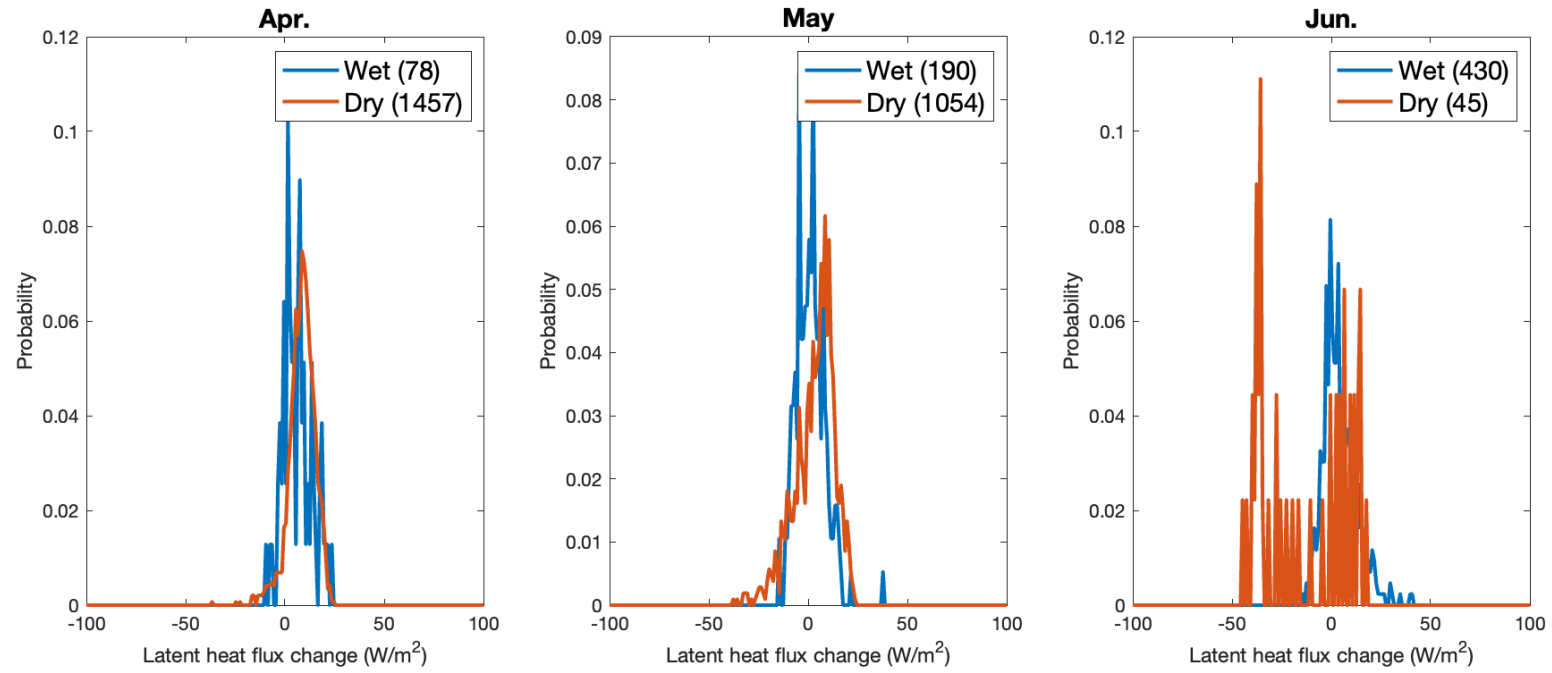


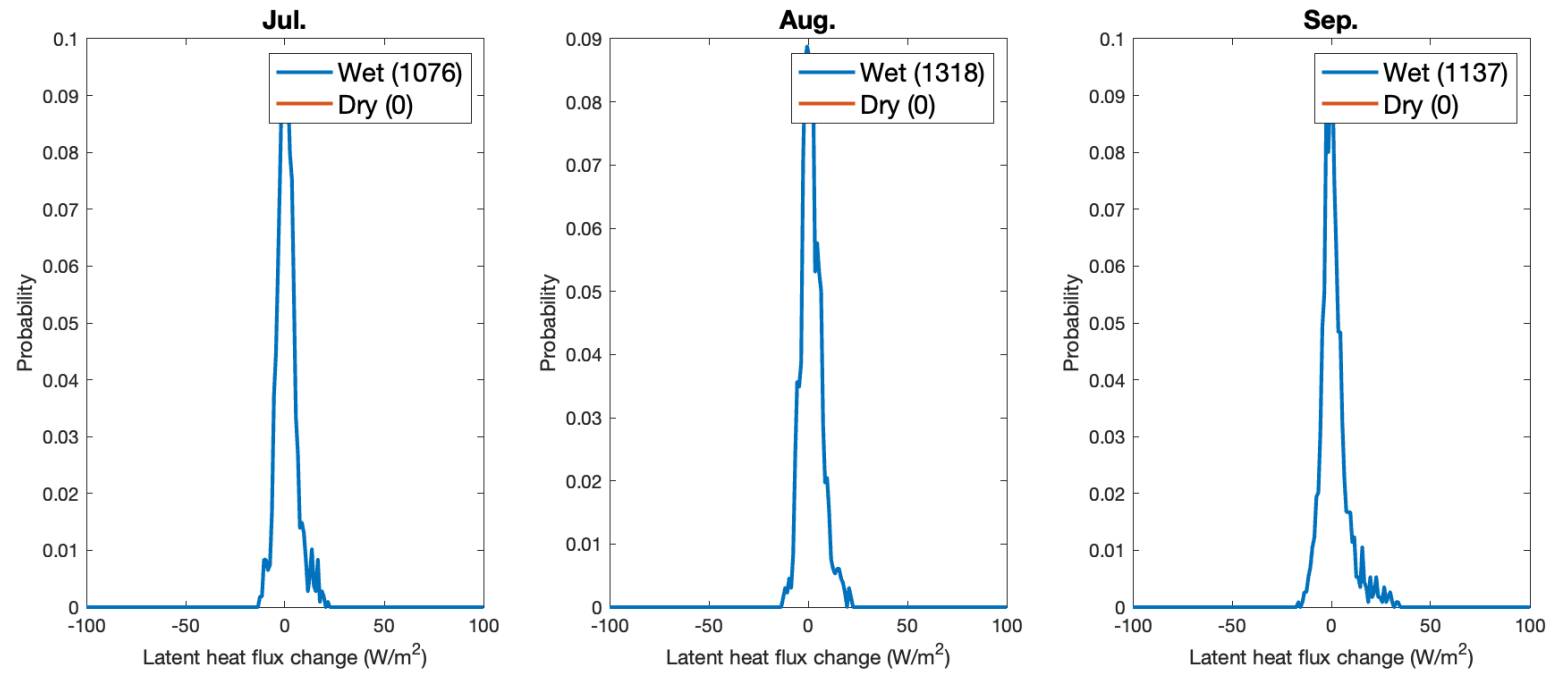
Figure 33. The summary of wet and dry conditions of wet-bulb temperature. The red route represents most of the scenarios for the dry condition.



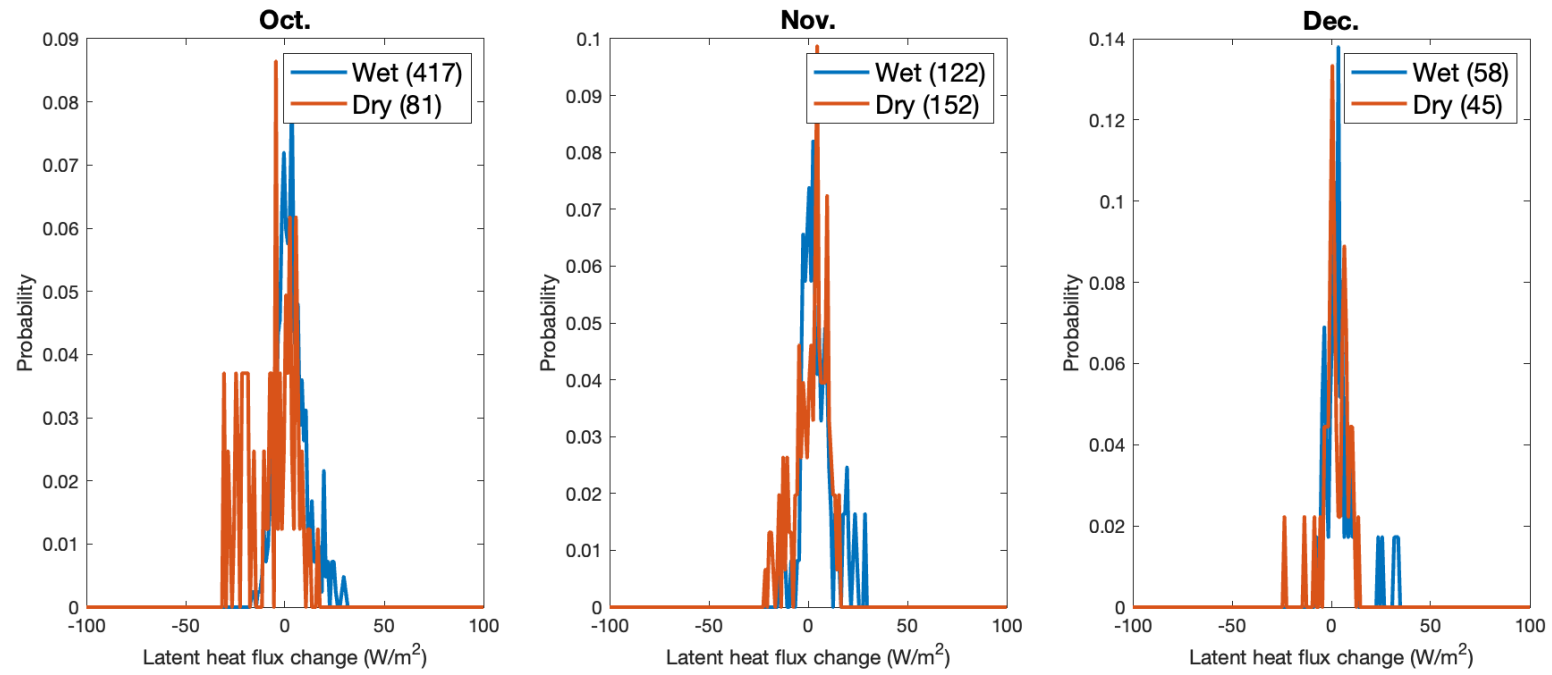
Appendix A1. The probability density function of dry and wet events from January to March in South Asia. The blue and red lines represent the wet and dry conditions. The number in the parentheses denotes the number of monthly events from 1981 to 2010.



Appendix A2. Same as A1, but for April to June.



Appendix A3. Same as A1, but for July to September.



Appendix A4. Same as A1, but for October to December.